Simulating animal movement trajectories from temporally dynamic step selection functions

Scott W Forrest[1,2,3,*], Dan Pagendam[4], Michael Bode[1,2], Christopher Drovandi[1,2], Jonathan R Potts[5], Justin Perry[6], Eric Vanderduys[3], and Andrew J Hoskins[7]

[1]School of Mathematical Sciences, Queensland University of Technology, Australia
[2]Centre for Data Science, Queensland University of Technology, Brisbane, Australia
[3]CSIRO Environment, Dutton Park, Australia
[4]CSIRO Data61, Dutton Park, Australia
[5]School of Mathematics and Statistics, University of Sheffield, Sheffield, UK
[6]Northern Australian Indigenous Land and Sea Management Alliance, Darwin, Australia
[7]CSIRO Environment, Townsville, Australia
[*]Corresponding author: scott.forrest@qut.edu.au

March 19, 2024

Abstract

1. Context and purpose
There has been increasing interest in simulating stochastic movement paths from step selection models. Hitherto, models used to simulate trajectories have not included temporally dynamic coefficients on both the movement and external selection processes, despite animals having temporally dynamic behaviour over daily or seasonal timescales.

2. Approach and methods
Here, we focused on simulating stochastic trajectories from step selection functions (SSFs) that include temporal dynamics using harmonic terms, focusing on dynamic behaviour on a daily timescale. The models also incorporated home ranging behaviour through a decaying memory process, which was also interacted with the harmonic terms. We simulated trajectories of individual animals and assessed how they compared to observed data through animal-movement-informed summary statistics. We applied our methods to GPS-tracked water buffalo (*Bubalus bubalis*), which are an invasive species in Northern Australia's tropical savannas.

3. Main results
The temporally dynamic models allowed for more informative interpretation of animal behaviour, particularly when quadratic terms were included in the models, allowing for insights about buffalo behaviour. The simulations generated from the temporally dynamic models reproduced the movement and habitat selection behaviour that we observed in the GPS data, particularly crepuscular movement behaviour and selecting for high canopy cover and vegetation during the middle of the day for thermoregulation. When assessed over longer time-scales, models both with and without daily temporal dynamics generated simulations that performed similarly according to the summary statistics, and had geographical space use of similar area and monthly overlap to that the observed data.

4. Conclusions and wider implications
We recommend fitting temporally dynamic SSFs when generating simulated trajectories to most

closely represent the animal's dynamic behaviour. We considered daily behavioural dynamics here, although any timescale of interest can be incorporated, with the potential for interacting multi scale temporal dynamics. Including temporal dynamics in SSFs for the purpose of simulating new data can address a wide range of ecological and behavioural questions and provide valuable information for conservation management, particularly for species with clear daily or seasonal behaviour patterns. We provide code to replicate all analyses presented.

Keywords

animal movement, conservation management, harmonics, rhythmic behaviour, simulating trajectories, step selection functions, summary statistics, temporal dynamics

1 Introduction

The movement and distribution of animals across a landscape is the result of successive fine-scale behavioural decisions. These complex decision-making processes relate to extrinsic factors such as resources, weather and other animals, and intrinsic factors such as age, sex, memory and energetic state (Turchin, 1998; Nathan et al., 2008; Fagan et al., 2013). These movement and habitat selection behaviours also change throughout time across various scales, which often predictably relate to natural cycles. Animals typically have daily rhythms that mediate foraging or hunting behaviours, resting, and finding water, and often have seasonal rhythms determined by the availability of resources and breeding behaviour (Tulloch, 1970; Ager et al., 2003; Rafiq et al., 2023). Predicting how animals move and distribute across a landscape can provide critical information when planning spatially-dependent conservation management actions (Guisan & Thuiller, 2005; Guisan et al., 2013; Guisan et al., 2017; Forrest et al., 2022), and incorporating temporal dynamics can lead to more accurate predictions.

Step selection functions (SSFs) are statistical models commonly applied to telemetry data to infer movement behaviour and habitat selection (Fortin et al., 2005; Potts et al., 2014; Thurfjell et al., 2014; Avgar et al., 2016; Northrup et al., 2022; Potts & Börger, 2023; Michelot et al., 2024). The SSF combines two terms, one of which describes the movement behaviour of the animal, and the other describes how animals select areas of the landscape (Forester et al., 2009; Potts et al., 2014; Arce Guillen et al., 2023). The external selection term describes the association between the animal and any covariates that represent the surrounding landscape (Fortin et al., 2005; Thurfjell et al., 2014). We use the term 'external selection' rather than 'habitat selection' as this model component can include other factors such as conspecifics, predator or prey density, intensity of previous space use, or any other covariates that can be represented spatially (Oliveira-Santos et al., 2016; Potts, Börger, et al., 2022; Potts & Börger, 2023; Michelot et al., 2024). To denote the SSF, p is the likelihood of observing an animal at location s_t given its last two observed locations s_{t-1}, s_{t-2} with locations indexed by discrete time t and within a spatial domain S. Let $\mathbf{X}$ be a multivariate spatial field indexed by a location s_t, and where $\mathbf{X}(s_t) = (X_1(s_t), \ldots, X_n(s_t))$ is a vector with a length equal to the number of spatial covariates:

$$p(s_t|s_{t-2}, s_{t-1}; \boldsymbol{\beta}(\tau;\boldsymbol{\alpha}), \boldsymbol{\theta}(\tau;\boldsymbol{\alpha})) = \frac{\phi(s_{t-2}, s_{t-1}, s_t; \boldsymbol{\theta}(\tau;\boldsymbol{\alpha}))\omega(\mathbf{X}(s_t); \boldsymbol{\beta}(\tau;\boldsymbol{\alpha}))}{\int_{q_t \in S} \phi(s_{t-2}, s_{t-1}, q_t; \boldsymbol{\theta}(\tau;\boldsymbol{\alpha}))\omega(\mathbf{X}(q_t); \boldsymbol{\beta}(\tau;\boldsymbol{\alpha}))dq_t}, \quad (1)$$

Here, ϕ denotes the movement kernel, with parameters relating to step lengths and turning angles contained in $\boldsymbol{\theta}(\tau;\boldsymbol{\alpha})$, which may be some function of time which we denote here as τ, as this time component may be cyclic and therefore not be equal to the absolute time, t. The parameter vector $\boldsymbol{\alpha}$ defines the functional relationship between $\boldsymbol{\theta}$ and τ. The ω component is the external selection kernel, and the term in the denominator ensures that the probability density, $p(\cdot)$, integrates to 1, which in practice is typically approximated through numerical integration, where we sample a set of proposed next steps given what is 'available' to the animal as determined by the movement kernel (Avgar et al., 2016; Michelot et al., 2024). Within the external selection kernel, $\boldsymbol{\beta}(\tau;\boldsymbol{\alpha}) =$

$(\beta_1(\tau;\boldsymbol{\alpha}_1),\ldots,\beta_n(\tau;\boldsymbol{\alpha}_n))$ is a vector of coefficients that may also have a functional relationship with τ defined by parameter vectors $\boldsymbol{\alpha} = (\boldsymbol{\alpha}_1,\ldots,\boldsymbol{\alpha}_n)$, where the ith coefficient, $\beta_i(\tau;\boldsymbol{\alpha}_i)$ is parameterised by parameter vector $\boldsymbol{\alpha}_i$ and corresponds to the ith spatial covariate in $\mathbf{X}$.

The external selection term is typically modelled analogously to a resource-selection function (RSF), that assumes an exponential (log-linear) form as:

$$\omega(\mathbf{X}(s_t);\boldsymbol{\beta}(\tau;\boldsymbol{\alpha})) = \exp(\beta_1(\tau;\boldsymbol{\alpha}_1)X_1(s_t) + \cdots + \beta_n(\tau;\boldsymbol{\alpha}_n)X_n(s_t)). \tag{2}$$

There are multiple ways to define the functional relationships between the parameter vectors $\boldsymbol{\beta}$ and $\boldsymbol{\theta}$ and τ (i.e. to incorporate temporal dynamics into SSFs), and one of the popular approaches is through harmonic terms (Ager et al., 2003; Forester et al., 2009; Tsalyuk et al., 2019; Richter et al., 2020). Harmonics are a natural choice as they are cyclical, which often aligns with temporal changes that animals respond to, such as daily or seasonal cycles (Boyce et al., 2010), although other additive terms, such as splines, are another obvious choice (Hanks et al., 2015; Klappstein et al., 2024). Harmonics are pairs of sine and cosine terms that have cyclic periods of varying frequency, such as $\sin(2\pi\tau/T)$ and $\cos(2\pi\tau/T)$, where $\tau \in T$. For a yearly cycle for instance, τ would represent the day of the year, and T would equal 365, although τ does not need to be integer-valued, and can be arbitrarily fine. The functional form of the relationship between $\boldsymbol{\beta}$ and τ when including harmonics would be:

$$\beta_i(\tau;\boldsymbol{\alpha}_i) = \alpha_{i,0} + \sum_{j=1}^{P} \alpha_{i,j} \sin\left(\frac{2j\pi\tau}{T}\right) + \sum_{j=1}^{P} \alpha_{i,j+P} \cos\left(\frac{2j\pi\tau}{T}\right), \tag{3}$$

where $\boldsymbol{\alpha}_i = (\alpha_{i,0},\ldots,\alpha_{i,2P})$, and P denotes the number of pairs of sine and cosine terms.

Recently, SSFs have been gaining popularity for generating predictions, both for estimating utilisation distributions (UDs) of an individual (or set of individuals) in a given area (Signer et al., 2017; Potts, Börger, et al., 2022; Signer et al., 2023) and for predicting conservation-relevant measures such as connectivity and movement corridors (Osipova et al., 2019; Hooker et al., 2021; Whittington et al., 2022; Aiello et al., 2023; Hofmann et al., 2023; Sells et al., 2023). Using the estimated parameters of an SSF, several approaches have been developed to generate predictions, which include analytic and simulation-based approaches (Barnett & Moorcroft, 2008; Avgar et al., 2016; Signer et al., 2017; Potts & Schlägel, 2020; Potts, Börger, et al., 2022; Potts, Giunta, et al., 2022). For a review of approaches to 'scale-up' from step selection functions to spatiotemporal patterns, see Potts and Börger (2023). A flexible and robust approach that allows for several prediction outcomes is to generate trajectories from the inferred parameters of the SSF via stochastic simulation (Avgar et al., 2013; Duchesne et al., 2015; Avgar et al., 2016; Signer et al., 2017; Potts & Börger, 2023; Signer et al., 2023).

There have been a number of recent studies generating stochastic trajectories for assessing conservation-relevant measures such as connectivity (Osipova et al., 2019; Hooker et al., 2021; Whittington et al., 2022; Aiello et al., 2023; Hofmann et al., 2023; Sells et al., 2023), although these simulations have not considered continuous temporal dynamics on both the movement and external selection processes. To contribute towards this emerging approach, we incorporate continuous temporal dynamics into the movement, external selection and memory processes of SSFs, for the specific goal of generating trajectories. We assess the utility of including temporal dynamics by comparing trajectories from SSF models with and without temporal dynamics against the observed data using a set of animal-movement-informed summary statistics. We also provide novel visualisations of the model fits with temporal dynamics and quadratic terms, and present a set of summary statistics similar to Abrahms et al. (2017) and Kays et al. (2023) that we use to compare between observed and simulated trajectories. As a case study, we fit temporally dynamic SSF models to introduced Asian water buffalo (*Bubalus bubalis* - hereafter buffalo) in the monsoonal ecosystems of Northern Australia. Buffalo cause significant environmental degradation in Northern Australia (Braithwaite et al., 1984; Skeat et al., 1996; Werner, 2005; Mihailou & Massaro, 2021), as well as harbour economically significant diseases (Skeat et al., 1996; Robinson et al., 2005; Petty et al., 2007). Management actions such as mustering and aerial shooting are inherently spatially dependent, and

accurately predicting where buffalo will be at any given time is of key importance. However, the methods we present here are not restricted to any particular species and are intended to be widely applicable.

2 Methods

2.1 Data collection and preparation

Asian water buffalo (*Bubalus bubalis*) location data from GPS-tracking were collected in collaboration with rangers in the Djelk Indigenous Protected Area in Arnhem Land, Northern Territory, between July 2018 and November 2019. Due to their size and potential risk to handlers, wild buffalo were immobilised via a helicopter using tranquiliser darts following a modified version of the methods described in McMahon and Bradshaw (2008). All anaesthesia procedures on buffalo were undertaken by a qualified wildlife vet. Animals were equipped with a device that was a combination of a commercial VHF tracking collar (Telonics MOD-500) and a custom developed LoRa (long-range) radio enabled GPS tracking pod. In total the VHF collar and LoRa-GPS pod weighed 1.2 kg. The LoRa-GPS pods were scheduled to collect a GPS location once an hour with an accuracy of 10 m, and attempted to transmit GPS locations over a custom-installed LoRa network. GPS locations were also logged onboard the device, which is the data that was used in this study. In total 17 female buffalo were GPS-tracked, all devices were retrieved, and of those we used 13 individuals that had high-quality data with temporally consistent fixes for at least 3 months. The hourly GPS locations had a high fix-success rate of 88% on average (range = 59% - 95%). To generate 'available' steps for the step selection numerical integration (Michelot et al., 2024), we fitted a Gamma distribution to the observed step lengths and a von Mises distribution to the observed turning angles of all individuals (Fieberg et al., 2021), and sampled independently from these distributions to generate new steps. We matched each observed step with 10 randomly-generated available steps.

2.2 Landscape covariates

Buffalo's movement decisions are driven by factors such as vegetation composition and density for resource acquisition and shade, access to water, and the terrain (Campbell et al., 2020). In monsoonal ecosystems of Northern Australia, vegetation and the distribution of water changes dramatically throughout the year. To represent the seasonal changes in vegetation, we used monthly Normalised Difference Vegetation Index (NDVI), which was derived from Sentinel-2 remote sensing data and measures photosynthetic activity and approximates the density and health of vegetation (Reed et al., 1994; Myneni et al., 1995; Campbell et al., 2020). Monthly NDVI layers were generated using Google Earth Engine using the clearest pixels from a range of images for that month to alleviate the effects of obstruction from clouds. We selected the highest quality-band-score, which is based on cloud and shadow probability for each pixel, resulting in a single obstruction-free image of the NDVI values for each month of each year. We also used temporally-static layers for canopy cover and herbaceous vegetation, which were derived from Landsat. We represented the terrain by including a slope covariate, which was summarised from a digital elevation model using the 'terra' package (Hijmans, 2024), and was calculated using the methodology of Horn (1981). The canopy cover layer was a proportion from 0 (completely open) to 1 (completely closed), and the herbaceous vegetation layer was binary, with 1 representing grasses and forbs, and 0 representing other (which is predominately woody growth). All spatial variables were discretised into grids (i.e. rasters) comprised of 25 m x 25 m cells.

2.3 Memory process - previous space use density

Including a covariate that allows for a tendency to return to previously visited locations, which represents a memory process, is becoming more common in step selection models and is known to provide less-biased inference on external selection parameters when there is a clear site-fidelity

or home range behaviour (Schlägel & Lewis, 2014; Oliveira-Santos et al., 2016; Rheault et al., 2021). We incorporated location history through the density of previous locations, which is similar to the approaches of Oliveira-Santos et al. (2016) and Rheault et al. (2021). We used kernel density estimation (KDE) to estimate the utilisation density (UD) of previous locations, which we combined with a temporal decay component. KDE UDs do not consider the autocorrelation present in the GPS data (Fleming et al., 2015), but they are computationally efficient, and are practical to use in a simulation model where the previous space use density must be updated at every simulated time-step. The temporal decay component is similar to the decaying parameter function of $\frac{1}{1+k\times t}$ in Merkle et al. (2014) and Rheault et al. (2021), but the negative exponential decay parameter that we used initially declines slower and has a lighter tail. Either function is likely to be appropriate for most situations. For our approach, the density f at the current location $s_t = (x, y)$ and time t is defined by

$$f(s_t) = \frac{\sum_{i=1}^{n} \exp^{-\gamma(t-t_i)} K_\sigma(x - x_i) K_\sigma(y - y_i)}{\sum_{i=1}^{n} \exp^{-\gamma(t-t_i)}}, \tag{4}$$

where previous locations are indexed by $i = 1, \ldots, n$, where n represents the number of locations that are considered in the previous space use density estimation. The γ parameter defines the strength of temporal decay, t_i is the time of each previous location, and x_i and y_i are the spatial coordinates of each previous location. The kernel function K_σ is a Gaussian density where $K_\sigma(d) = \frac{1}{\sigma\sqrt{2\pi}} e^{-\frac{1}{2}(\frac{d}{\sigma})^2}$, where d is the distance in the x or y direction, and σ is the standard deviation, i.e. the bandwidth parameter of the KDE (which is often denoted by h). The denominator normalises over the temporal decay component. Similarly to Rheault et al. (2021), we excluded locations from the past 24 hours, as these locations are likely to reflect the autocorrelation in the movement process rather than resulting from a memory process.

We used the observed data to estimate the σ parameter with the normal or 'reference' bandwidth estimator over all used points using the `amt` package (Worton, 1989; Gitzen et al., 2006; Kie, 2013; Signer & Fieberg, 2021), and σ was estimated separately for each individual. Although the reference bandwidth is known to oversmooth locations (Gitzen et al., 2006), when used in an SSF model that will be used to generate trajectories the oversmoothing may be preferable, as the previous space use density represents a general familiarity with particular areas. In contrast, the kernel bandwidth when using the plug-in estimator (Sheather & Jones, 1991) was very small, resulting in numerous small and fragmented modes in the distribution, which may conflate with particular specific locations and dilute the influence of habitat in the model, leading to poorer external selection inference overall.

As we intended to fit population-level (hierarchical) models, we wanted a single KDE bandwidth parameter, $\bar{\sigma}$, and a single temporal decay parameter, γ_{pop}. Therefore, after estimating the σ parameter for each individual, we took the mean, $\bar{\sigma}$, and estimated a single, 'population-level' γ_{pop} parameter for all individuals using maximum likelihood estimation, resulting in population level memory parameters. This process could also be done separately for each individual, and in Appendix A we show the results of individual-level and population-level σ and γ parameter estimation. For the maximum likelihood estimation of the γ parameters (fitted to each individual as well as to all individuals) we used the 'L-BFGS-B' method in the R 'optim' function as it allows for box constraints, and we used 0 and 1 for the lower and upper constraints of the γ and γ_{pop} parameter.

2.4 Model fitting and temporally-varying parameters

Buffalo have temporally dynamic patterns in their movement and external selection behaviours across two predominant time-scales; daily and seasonal. Daily rhythms are predominately driven by daylight and temperature, and seasonal rhythms are predominately driven by the distribution of water and the availability of forage (Tulloch, 1970; Campbell et al., 2020). Seasonal behaviours of water buffalo have already been studied in some detail, so we investigated how buffalo movement and external selection behaviours change on a daily time-scale. Due to the presence of seasonal patterns, we separated data into wet and dry seasons and fitted independent wet and dry sea-

son models with daily behaviour. An extension of this work would be to incorporate multiple interacting time-scales, such as daily rhythms that also change across the seasons.

To incorporate the temporal dynamics on a daily time-scale, each movement parameter and environmental covariate was included in the model as a linear predictor as well as interacting with pairs of harmonic terms relating to the hour of the day (Forester et al., 2009; Street et al., 2016; Tsalyuk et al., 2019; Warton, 2022). The resulting set of harmonics that we selected from to fit models was $\sin(2k\pi\tau/24)$ and $\cos(2k\pi\tau/24)$ for $k = 1, 2, 3$, where τ is indexed by the hour of the day, resulting in models with up to three pairs of sine and cosine terms. Each movement parameter and spatial covariate (including previous space use density) has therefore up to seven estimated parameters, which can be reconstructed into a single function that varies across the day. To allow for external selection to operate over a region of the environmental space (rather than monotonically increasing or decreasing), we also included quadratic parameters for NDVI (i.e. NDVI^2), canopy cover and previous space use, which were also interacted with the harmonic terms. To assess the value of including temporal dynamics, we fitted models with increasing numbers of harmonics, from 0 pairs (static model), to 1, 2 and 3 pairs (dynamic models), which we denoted as 0p, 1p, 2p and 3p, respectively.

Due to the large number of covariates when including several pairs of harmonics, particularly when also including quadratic terms, we had difficulty fitting population-level models with the 'glmmTMB' (Brooks et al., 2017) and 'INLA' (Rue et al., 2009) model fitting approaches (Muff et al., 2020). We therefore fitted models to all individuals using the 'TwoStep' approach (Craiu et al., 2011, 2016) which can be considered as a more computationally efficient alternative, providing certain conditions are met. For a more detailed comparison see Muff et al. (2020). For computational stability, prior to model fitting we centred and scaled all variables by subtracting mean values and dividing by the standard deviation, using the data from all used and random steps. The centering and scaling was immediately prior to model fitting, and therefore after multiplying the covariates with the harmonics. In practice, this was achieved by creating a design matrix of all covariates and interactions (with harmonic terms), and then centering and scaling the design matrix (with respect to each of the covariates). Following model fitting, the coefficients and covariates were returned to their natural scale for interpretation and prediction.

2.5 Generating trajectories from the fitted model

We generated trajectories by replicating the step-selection approach. A starting location is selected from the domain, which in our case was typically the first location of an observed trajectory for comparison, and n random steps are drawn from the 'selection-free' or 'updated' movement kernel (Fieberg et al., 2021) by sampling independently from the updated Gamma and von Mises distributions of step-lengths and turning angles for time τ, respectively. For each proposed step, $\exp\left(\boldsymbol{\beta}(\tau;\boldsymbol{\alpha})\mathbf{X}(s_t)\right)$ is evaluated, which includes the previous space use density using kernel density estimation with the temporal decay over the previous locations (Equation 4). This results in a value for each step that is proportional to the probability of being selected, and a single step is selected weighted by these probabilities. This new step is added to the trajectory and becomes the starting point for the next step, and the process is repeated until the specified number of steps are reached.

As the memory process depends on previous locations, and the simulations start with a single point, the previous space use must be built up during a 'warm-up' period. To achieve this, we had two distinct periods within the simulation; for the first 48 hours of the simulation (double the memory delay), all of the previous locations are weighted equally to ensure that the simulated animal has some attraction at the initial location and stays in the general area. For the remainder of the simulation the memory delay and the temporal decay are included, and the previous space use density (excluding the most recent 24 hours) is defined by Equation 4. We truncated the number of locations that are included in the previous space use density calculations to 500 locations, as the temporal decay is near 0 at this point (Appendix A). At least 500 of the warm-up locations are then discarded from the trajectory (the exact number depends on the start time of the observed data).

Within the simulations, we proposed 50 steps at each time-step, and we ran the simulations for

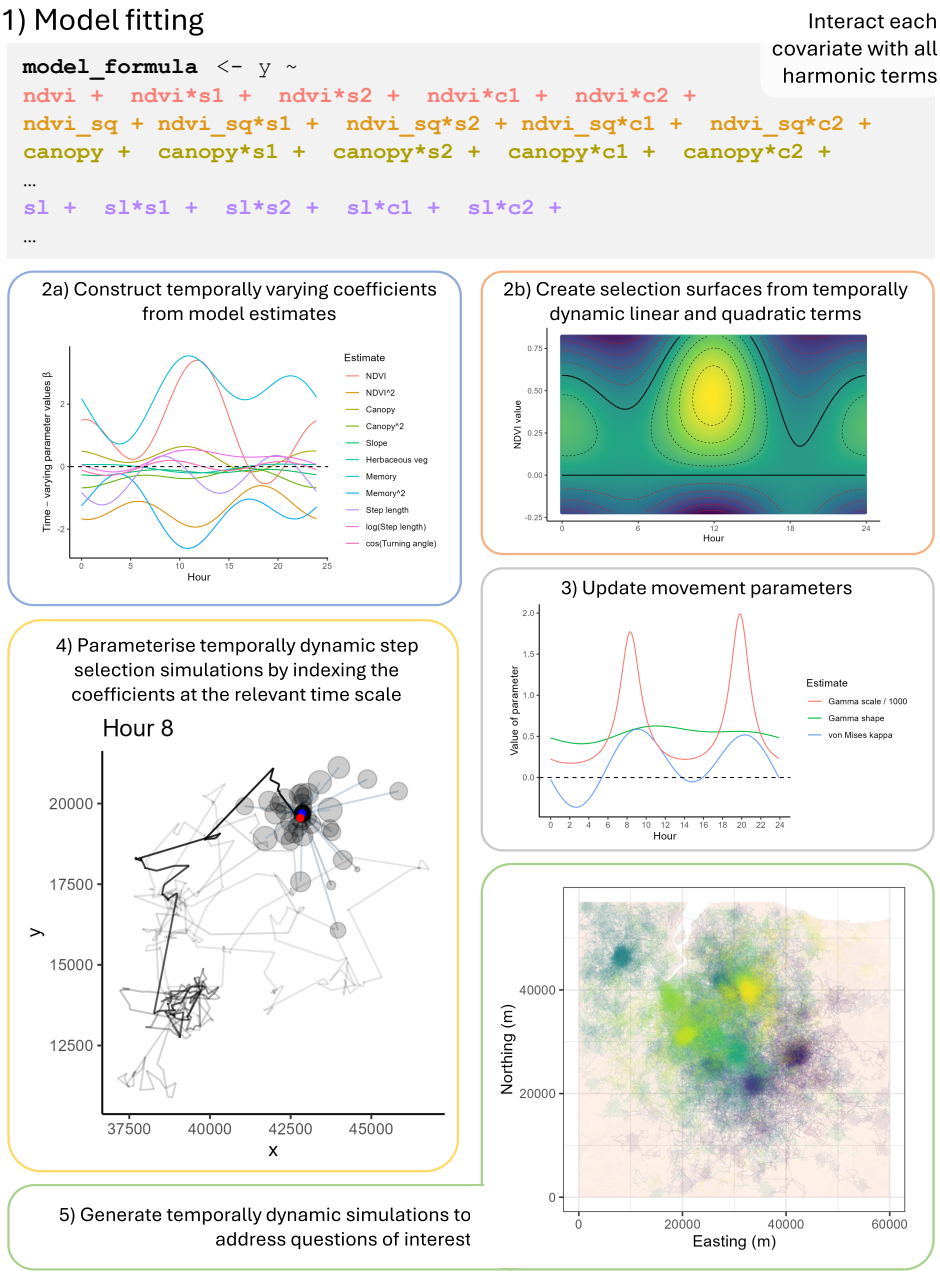

Figure 1: Concept plot illustrating the procedure of model fitting with harmonic terms, reconstructing the temporally dynamic coefficients, and generating temporally dynamic trajectories. The model is fitted with covariates interacting with the harmonic terms, where $s1$, $s2$, $c1$ and $c2$ in the model formula represent $\sin(2\pi\tau/24)$, $\sin(4\pi\tau/24)$, $\cos(2\pi\tau/24)$ and $\cos(4\pi\tau/24)$, respectively, where τ is the hour of the day and $\tau \in T$, with T denoting 24 hours. All covariates can be interacted with the harmonics, including quadratic terms, movement parameters and a memory covariate. The coefficients are then reconstructed into time-varying coefficients (2a), and when linear and quadratic terms are interacted with harmonic terms, 'selection surfaces' can be created (2b). The movement parameters are 'updated' following the typical procedure (Avgar et al., 2016; Fieberg et al., 2021), although this is performed across T (3). In our case there were negative values for the von Mises kappa parameter, suggesting that the mean of the distribution changed from 0 to π, indicating a higher likelihood of taking return steps. Using the temporally dynamic external selection coefficients and updated movement parameters, simulations can be run by indexing the coefficients and parameters at time τ (4). In (4), we have shown the proposed steps from the current (blue) point, with the size of the circle at the end representing the probability of choosing that step, based on the habitat covariates and previous space use density. The red circle was the step that was selected, and forms the starting point for the next step. An important point is that any time-scale of interest can be considered, such as seasonal time-scales, not just hourly as we have considered here.

enough locations to include a warm-up period for the memory process and to cover the duration of the observed data for the season of interest. The temporally dynamic coefficient values and the memory parameters (KDE bandwidth $\bar{\sigma}$ and temporal decay γ_{pop}) were the same across all simulated trajectories, and only the starting locations differed. We ran simulations from dry season models starting from when the GPS devices were deployed in late-July 2018, until the end of the 2018 dry season at the start of November, covering approximately a three-month period. For the purposes of interpretation and comparison, we ran 50 simulated trajectories from the starting locations of each of the 13 buffalo, and we subsequently removed simulated locations at times when the observed data was missing for that individual (typically due to failed GPS fixes), to maintain any temporal biases present in the data. Overall, that resulted in 650 simulated trajectories for each of the four models, with each trajectory between 1315 and 2220 locations, for an average of 2048 locations. Each simulated trajectory took approximately 5 minutes, which can be parallelised easily as each simulation is independent, with a significant proportion of computation time relating to the memory process, as the KDE density with temporal decay is estimated for all proposed steps at each time point.

2.6 Comparing models and validating trajectories

To assess whether the simulations could recreate the temporal habitat selection patterns that were exhibited by the buffalo, and how many pairs of harmonics this required, we assessed summaries of movement and habitat selection dynamically throughout the day. To achieve this we binned both the observed and simulated trajectories into the hours of the day, and took the mean, median and standard deviation of step lengths and the four habitat covariates - NDVI, canopy cover, herbaceous vegetation and slope.

To determine whether including temporal dynamics afforded more representative movement behaviour over the full trajectory, we summarised the observed and simulated trajectories using relevant animal movement metrics, resulting in a set of summary statistics (Avgar et al., 2015; Abrahms et al., 2017; Hauenstein et al., 2019; Kays et al., 2023). Following Kays et al. (2023), we selected summary statistics that we divided into categories relating to step metrics, path metrics and life-history metrics, but as we were fitting the models with habitat covariates, we also included a fourth category that we called habitat metrics, which assessed the distribution of locations in environmental space. A complete list of summary statistics is in Appendix C. Similar to Abrahms et al. (2017) and Kays et al. (2023), we performed a Principal Component Analysis (PCA) on all of the full-trajectory summaries to visualise overall differences of the summary statistics between the observed and simulated trajectories. We scaled and centred all summary statistics prior to fitting the PCA.

3 Results

For the dynamic models that included harmonic terms there was clear temporal variability throughout the day for the buffalo's movement and external selection parameters, in both the dry and wet seasons (Figure 2, 3 and 4). The buffalo's movement behaviour followed a crepuscular pattern, with high movement around dawn and dusk, and the estimated movement parameters of the dynamic models replicated the pattern that was observed in the data (Figure 2). The external selection parameters indicated an avoidance of herbaceous vegetation (Figure 3) and selection of higher values of NDVI and canopy cover (Figure 4) during the middle of the day, which correlates with buffalo thermoregulation as they seek shelter from high temperatures and sun. There was also positive selection for herbaceous vegetation in the early morning and evening, which is likely to represent foraging periods (Figure 3). When the harmonic terms are not considered, the dynamics in relation to herbaceous vegetation average to a coefficient slightly below 0, obscuring the behaviour. The memory parameter also exhibited temporally dynamic patterns (Figure 4), with all dynamic models suggesting higher attraction to previous locations in the afternoon and evening, although the flexibility of different models resulted in slightly different trends.

The simulated trajectories from all models performed well in capturing the dynamics of buffalo

movement, with localised space use (i.e. home ranging behaviour) as well as more exploratory and wandering movements (Figure 5). The summary statistics of dynamic behaviour echoed the fitted model outputs, and indicated that the models with the temporal dynamics gave more accurate predictions of the buffalo behaviour when considered throughout the hours of the day (Figure 6). However, when considered across the entire trajectory, all models performed similarly for all sets of summary statistics (Appendix C), suggesting in our case that when predicting over longer time-scales the daily dynamics may not be essential to include in the models.

With respect to geographical space use or home ranges, each of the four models approximated the patterns observed in the buffalo data, both in terms of the area within the core and home range (50% and 95% contours of the KDEs, respectively) and monthly home range overlap (Appendix C). However, there was idiosyncratic variability between models, and we observed that models with zero or three pairs of harmonics (0p and 3p) were most accurate when considering the area contained within the 95% contour of the KDE home range, and the trajectories from models with one or three pairs of harmonics (1p and 3p) were most accurate when considering the space use overlap between months.

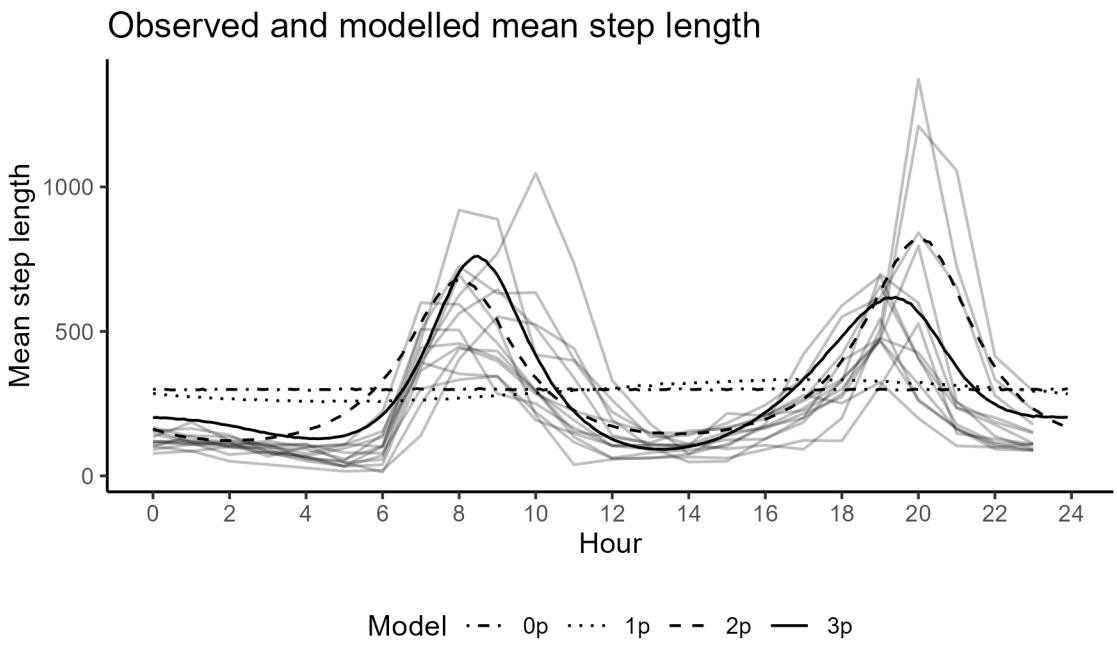

Figure 2: The observed and modelled mean step lengths across the hours of the day from all models when sampling from the estimated movement kernels. The observed mean step lengths are shown as a grey line for each individual. Samples from the estimated, temporally dynamic, step length distribution are shown with the black lines, with 0p, 1p, 2p and 3p referring to the number of pairs of harmonic terms included in the model. The movement parameters were updated using the estimated coefficients and the tentative Gamma and von Mises distributions that were fitted to the observed data and that random steps were sampled from prior to model fitting (Avgar et al., 2016; Fieberg et al., 2021; Michelot et al., 2024). The model with a single pair of harmonics is restricted to a single period, and fails to capture the two peaks of movement in the observed data. The 2p and 3p models are similar, although the model with three harmonics has more flexibility to represent the difference between the dawn and dusk periods of high activity.

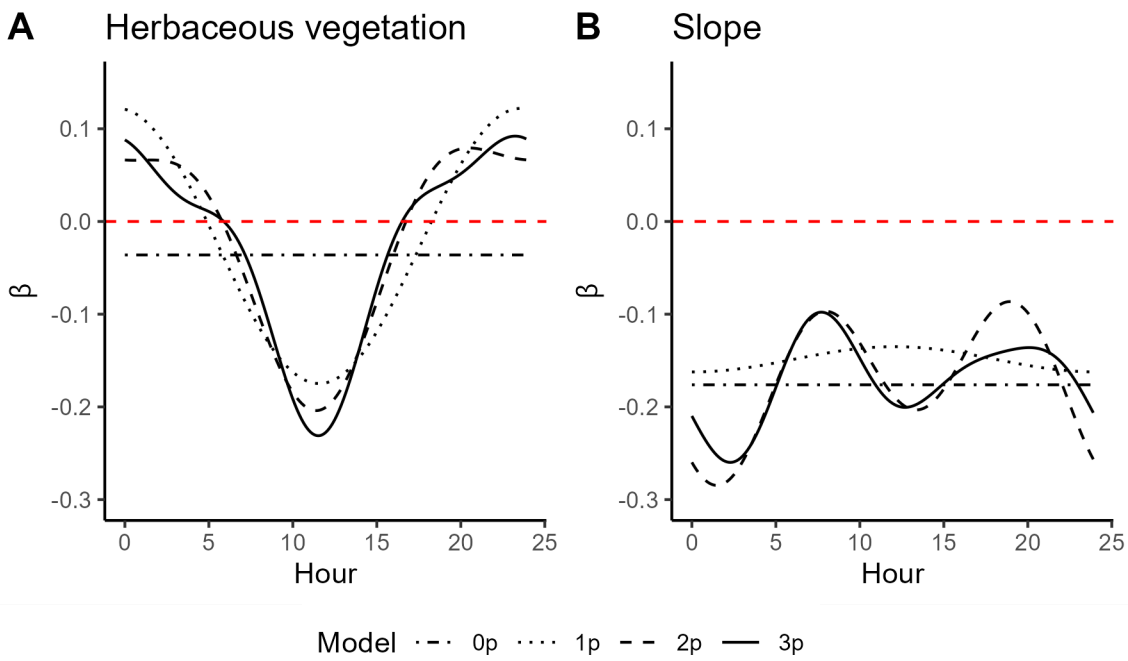

Figure 3: Estimated time-varying coefficients over the day for the external selection parameters of the population-level SSF model for 13 female buffalo in Arnhem Land, NT. Panel A shows the estimated coefficient for herbaceous vegetation for the four models. The static (0p) model averages over the effect throughout the day, suggesting incorrectly that there is little relationship to herbaceous vegetation. The dynamic models however reveal that there is attraction in the evening and avoidance during the day, as the buffalo seek shelter from the sun in woody vegetation. As there appears to be only a single period in this trend, all three dynamic models (1p, 2p and 3p) capture it. The trend for slope appears to have multiple modes, which is represented by the models with two and three pairs of harmonics.

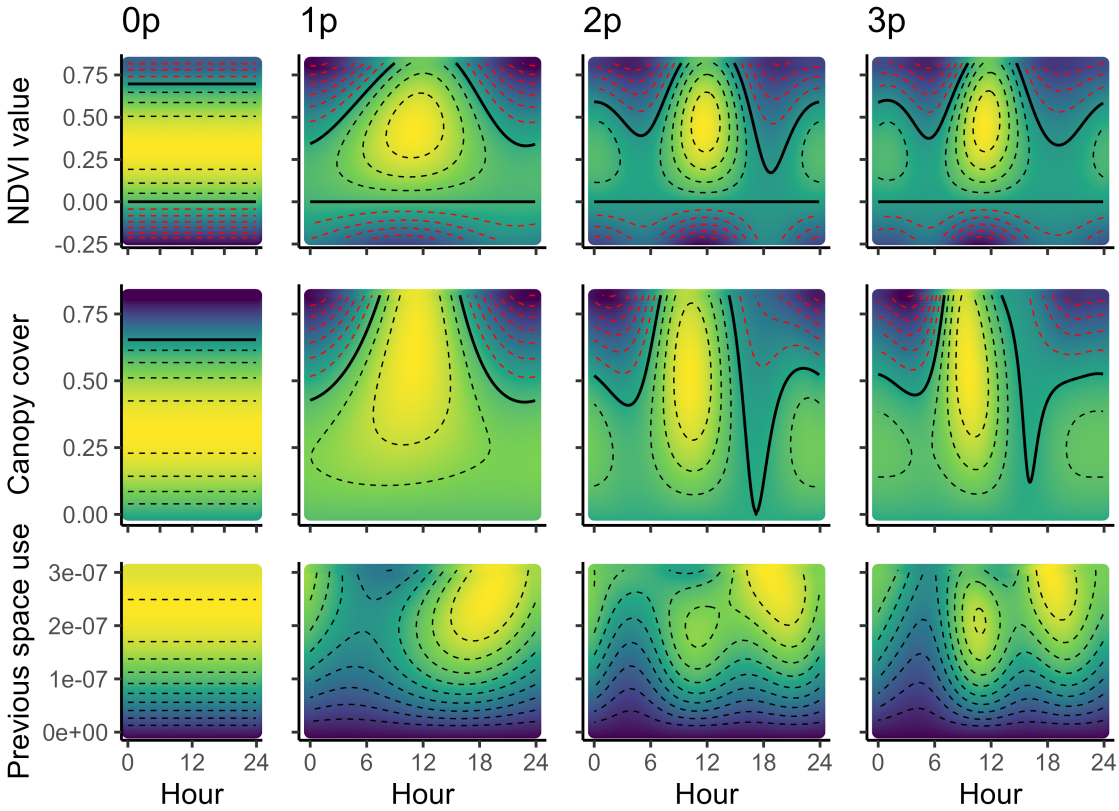

Figure 4: As there were both linear and quadratic terms that interacted with the harmonic terms for Normalised Difference Vegetation Index (NDVI), canopy cover and previous space use, it is possible to construct 'selection surfaces' that represent the strength of association on the natural scale of the covariate. The colours approaching yellow with the black dashed lines indicate positive selection with an estimated β coefficient above 0, with the solid black line showing the zero contour, and colours approaching purple with red dashed contours showing avoidance of those values of each covariate at those times. Due to the difference in scales of the covariates, the selections colours are scaled for each plot, and it should be noted that the values for the previous space use covariate (all models) are greater than 0. Each column represents a model with numbers of harmonics that increase to the right (0p, 1p, 2p and 3p denote 0, 1, 2 and 3 pairs of harmonics, respectively. Each row represents a different covariate within that model. For NDVI (top row) and canopy cover (second row), the models with one, two and three pairs of harmonics (1p, 2p and 3p) are similar, suggesting that increasing the number of harmonics is unlikely to change the model fit and therefore simulation outputs. For previous space use, the model fit for each number of covariates is different, suggesting that the increasing flexibility of the models attempt to capture more of the complicated memory process, and may benefit from even more harmonics or a different functional form (such as 2D splines - Klappstein et al. (2024)). The NDVI selection surface suggests that buffalo have an attraction for intermediate values of NDVI in the middle of the day, and selection against high values in the dawn and dusk periods, possibly to ease transit. The selection surface for canopy cover indicates that buffalo prefer denser canopy in the middle of the day (correlating with NDVI), suggesting that buffalo are seeking refuge for high temperatures and sun. The selection surface for previous space use indicates greater attraction to previous space use in the afternoon and evening, which may indicate an attraction to previously used areas for shelter or foraging, respectively.

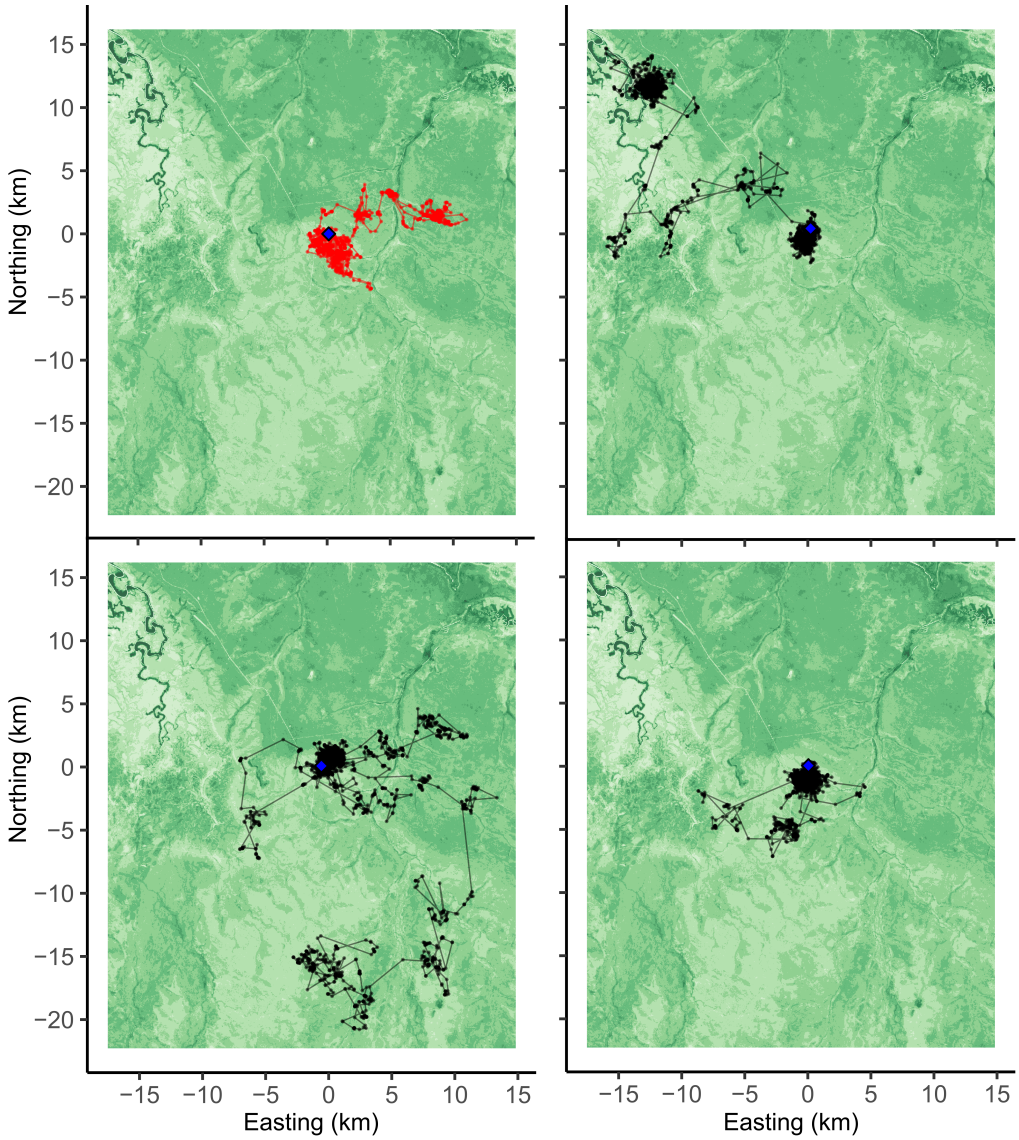

Figure 5: Trajectories of one buffalo (ID 2005 - shown in red) and three simulated trajectories (shown in black) generated from a fitted step selection model with two pairs of harmonics. The simulated trajectories started from the same initial location as the observed buffalo trajectory (set to 0,0 - shown as the blue point) and were run for the same number of locations, covering a three-month period in the late dry season 2018. The simulated trajectories required a 'warm-up' period for the memory process, and therefore after removing the warm-up period, there was typically some drift from the initial location. For comparison, we selected three simulated trajectories that finished the warm-up period near the initial starting location. Even with a relatively simplistic short-term memory process, the simulated trajectories capture the localised space use of the buffalo, but also allow for the wandering and relocation behaviour due to the temporal decay component of the previous space use.

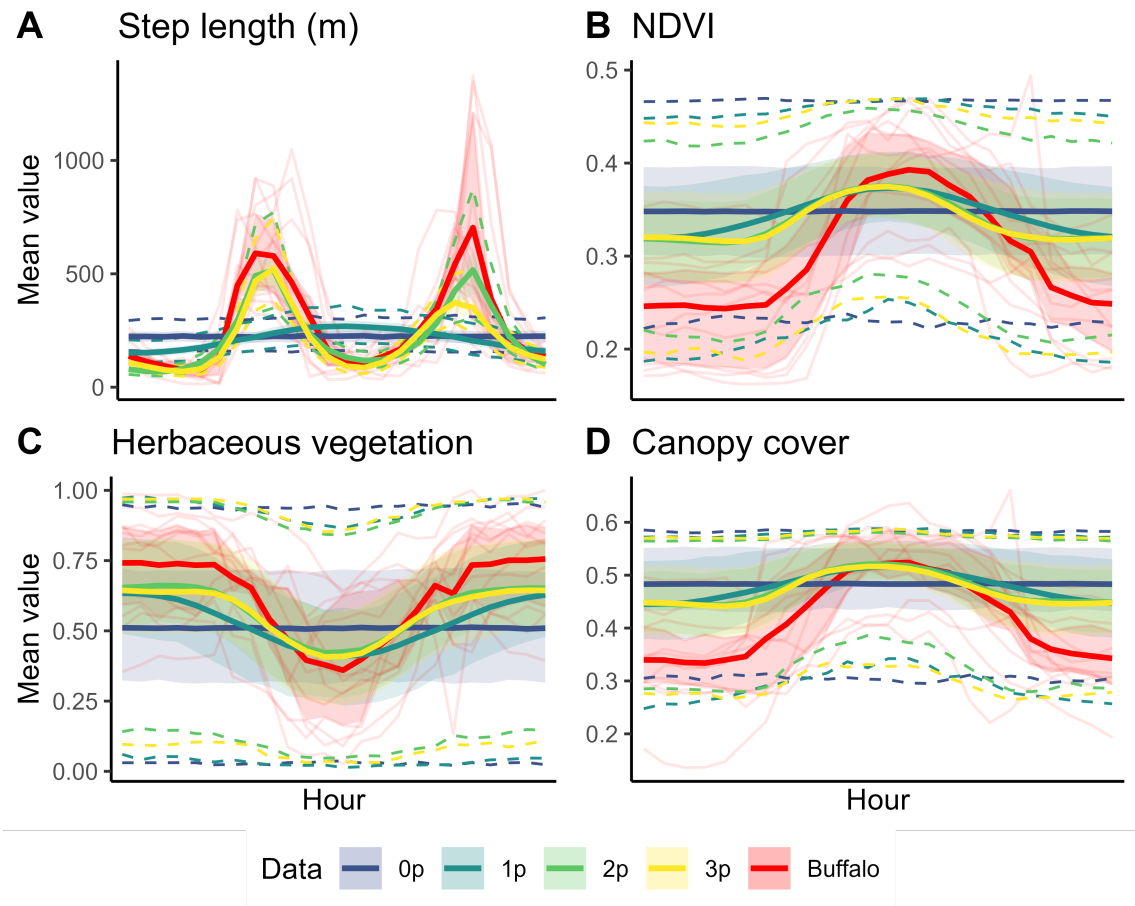

Figure 6: To assess the habitat selection of the simulated trajectories through time, we binned the trajectories into the hours of the day, extracted the values of the movement parameters and covariates for each hour, and took the mean, median and standard deviation. Here we show the mean values for the observed data and the simulations from each of the four models through time for (A) step length, (B) Normalised Difference Vegetation Index (NDVI), (C) herbaceous vegetation and (D) canopy cover. The shaded ribbons enclose the 25% and 75% quantiles, and the dashed lines are the 2.5% and 97% quantiles. The solid line is the mean for that hour across all trajectories for the buffalo or for each of the models. The observed data is shown in red, with each light red line representing one buffalo ($n = 13$). The dashed lines for the 2.5% and 97% quantiles are not displayed for the observed data, as all buffalo individuals are shown. For step length in Panel A, the simulated trajectories of the step selection models with two or three pairs of harmonics (2p and 3p) captured the bimodal, crepuscular movement pattern in the observed buffalo data. For the external covariates NDVI, herbaceous vegetation and canopy cover in Panels B-D, the simulated trajectories of the temporally dynamic models with one, two or three pairs of harmonics (1p, 2p, and 3p) largely capture the unimodal pattern of habitat selection in the dry season, which is driven by sun and high temperatures during the middle of the day, leading to seeking shelter in denser, more closed vegetation. The pattern is consistent across the buffalo and within each model, although the variance is wide, likely due to the portion of the landscape that is available to the buffalo or the simulated trajectories.

4 Discussion

In this study we incorporated temporal dynamics into SSFs for the purpose of generating simulated trajectories of water buffalo (*Bubalus bubalis*). Including temporal dynamics in trajectories allowed for realistic behaviour that replicated the temporal dynamics observed in the real data. The flexible, temporally dynamic responses in the estimated step selection parameters also revealed daily patterns of buffalo movement and external selection behaviour, particularly when quadratic terms were included in the model that allowed selection surfaces to be created for habitat selection and the memory process. The finer-scale summary statistics suggested that the dynamic models more accurately captured the daily behaviours of buffalo, although when considering the full trajectories that were several months long, these movement and habitat selection behaviours appeared to average out, suggesting that considering fine scale daily dynamics may not be important when predicting over longer time-scales. This particular finding may not generalise to other species however, particularly those that have greater mobility (e.g. flighted species) that can cover large distances within a day which may lead to substantially variable distributions throughout different periods of the day.

For some step selection processes, such as the external selection of NDVI, canopy cover and herbaceous vegetation, the responses exhibited a single mode of selection, and all dynamic models (denoted 1p, 2p and 3p for the number of harmonic pairs) largely captured this. However, for other processes such as the movement behaviour and the selection of slope and previous space use density, there were multimodal patterns which were only captured by the more flexible models (2p and 3p) that allowed for multiple modes. It is possible to identify the trend of temporal dynamics through the dynamic summary statistic approach we took for the step lengths and habitat covariates (Figure 6), which revealed the temporal dynamics of the buffalo and can be done as an exploratory step prior to any model fitting. Unlike the model fits for the four habitat covariates (NDVI, canopy cover, herbaceous vegetation and slope), the estimated coefficients of previous space use density, as indicated by the selection surfaces, did not appear to stabilise with increasing harmonics, suggesting that this process is more complicated and may require more flexibility from the responses. In this case we suggest trying more harmonics to capture the dynamics (at the expense of more computation and the risk of overfitting depending on the amount of data), or using a different functional form of the responses through spline terms or similar (Klappstein et al., 2024). The quadratic term may also not be flexible enough the capture the selection within the range of previous space use density, and 2-dimensional spline surfaces may be more useful. For the temporal dynamics, we also only considered a single time-scale in a model, such as daily *or* seasonal, rather than interacting both in the same model. Theoretically this is possible, and including daily harmonics that interacted with seasonal harmonics would give coefficients that are more realistic, although the number of parameters would increase, more data would be required, and the model would become more difficult to fit and to interpret.

It is important to note that simulation performance is sensitive to the form of the covariates. Here we included covariates that mostly range between -1 and 1 or between 0 and 1, and most of the environmental space is visited, limiting out of sample prediction. Covariates such as 'distance to' covariates can produce very different behaviour in simulations, as distances can become large, leading to very high or low selection behaviour which becomes apparent when simulating trajectories. In these cases we suggest considering transformations of the covariate, such as log-transformation, and we recommend quadratic terms in the models used for simulations, as it allows for the simulated individuals to select within a region of the covariates, rather than monotonically increasing or decreasing values as is the case when only considering linear terms. An example from our case is for NDVI (Figure 4), where even for the static (0p) model, selection is highest for NDVI values between 0.25 and 0.5, and there is avoidance for values less than 0 and greater than 0.7. Assessing the accuracy of simulations to different covariates is therefore important, and we suggest following a summary statistic approach as we have taken here, giving more weight to summary statistics that represent movement characteristics relating to the research question. An approach to assess the more qualitative aspects of the overall trajectory would be the 'lineup' approach (Fieberg et al., 2023), as many of the trajectories appeared visually similar to the observed data. We also advocate for using simulations as a means of model selection and to investigate drivers of animal movement decisions (Potts, Börger, et al., 2022).

The spatial memory of animals is a sophisticated process that is difficult to understand and to

model (Fagan et al., 2013; Schlägel & Lewis, 2014; Kim et al., 2023). The geographical space use of the simulated trajectories (i.e. home range) is also sensitive to the memory process of the models. Here we used a relatively simplistic memory process, and the results were sensitive to the estimated KDE bandwidth, the presence and parameterisation of the memory decay, and whether a quadratic term is included for the previous space use density in the models. Memory processes that have different forms, such as time since last visit (Schlägel & Lewis, 2014), or a multi-layer approach that has memory layers relating to food acquisition, mate finding and territory defence suggested by Fagan et al. (2013) will also give different results. These may also require (and can accommodate) different model specification. Careful thought should be given to the memory process that is included in step selection models, and we argue (along with other authors) that simulations provide a valuable method to uncovering the process of animals spatial memory (Merkle et al., 2014; Schlägel & Lewis, 2014; Merkle et al., 2017; Merkle et al., 2019; Thompson et al., 2022).

To highlight the influence of temporal dynamics we opted for a simple base model that has only movement, habitat selection and memory processes, although there are additional parameters that could be included to increase the realism of the simulated trajectories. We ignored the influence of conspecifics resulting in social dynamics, despite the fact that they are influential to animal movement (Potts, Börger, et al., 2022; Ellison et al., 2024). In part this was a decision made with respect to our data, as individuals from mostly separate clans were GPS-tagged, resulting in little observable influence between individuals. However, interacting covariates relating to conspecifics with temporal dynamics may lead to realistic patterns of social behaviour throughout the time-scale of interest, as there are likely to be fluctuations of attraction and repulsion to other individuals, for instance those that produce fusion-fission dynamics (Haydon et al., 2008; Silk et al., 2014; Le Goff et al., 2023). These fluctuations of social dynamics may relate to longer time-scales such cycles of breeding, although there may be fine-scale temporal dynamics that influence movement within a daily period.

We also did not consider parameter uncertainty of the model outputs in our simulations. This would be computationally expensive (as many more simulations would be required), although it would be straightforward to achieve, particularly if using a Bayesian sampling approach such as Markov Chain Monte Carlo (MCMC) to fit the models. In that case, samples could be drawn from the joint posterior and passed to the simulation procedure, essentially resulting in posterior predictions of animal movement trajectories (McElreath, 2020). For studies where predictions are generated to assess a research question such as distribution or connectivity, incorporating this uncertainty may be important, particularly if models are fitted hierarchically and one wants to consider the individual variability of spatial behaviours (Dall et al., 2012; Bastille-Rousseau & Wittemyer, 2019, 2022; Stuber et al., 2022). An alternative approach to consider individual variability is to fit models to each individual animal separately, which can each be used to simulate many trajectories. However in our case, fitting models to individuals separately led to pathological behaviour in the movement parameter updating process, which resulted in impossible movement kernels in some cases. For a more in-depth discussion see Appendix B.

In the models presented in this paper we used harmonic terms to incorporate the temporally dynamic behaviour in the simulations. However, a recent paper by Klappstein et al. (2024) shows that splines are another option, which also allow for SSF extensions and hierarchical model fitting using the `mgcv` package (Wood, 2011). Simulating trajectories from dynamic models fitted with spline terms would be the same process as we have presented here, and is just a matter of indexing the coefficients for $\tau \in T$ when simulating trajectories. It would also be possible to fit the two-dimensional selection surfaces using interacting spline terms that we achieved by interacting quadratic terms and harmonics, which would be more flexible than our approach, although it would add more parameters in the model and require more data to fit, but there appears to be promising potential in this area for parameterising simulations. Another alternative method of incorporating temporal dynamics into animal movement models is through state-switching (McClintock et al., 2012), and recently, state-switching models have been combined with SSFs (Klappstein et al., 2023; Pohle et al., 2023). Whilst these models can provide valuable information about the animal's behavioural states, such as when and where this occurs, state-switching is discrete, and is limited when behaviour changes are gradual and continuous. Using temporal dynamics allows for behavioural changes that are continuous, and behaviours may change in relation to their movement, habitat selection, or relationship to previous locations. Where behaviours switch quickly however, such as switching from resident to dispersing, or post-release behaviour (Picardi et al., 2021), then

state-switching models may provide more accurate simulations. We expect that both approaches would be useful to determine the nature of an animal's behaviour, and to assess whether their behaviours change gradually or rapidly, or whether there is some combination of both.

Simulated trajectories of animal movement have applications beyond what is possible compared to analytic prediction approaches such as resource selection functions (Potts & Börger, 2023), and we see many potential applications of using SSFs to generate trajectories, particularly when they can capture realistic movement dynamics. A promising application is for counter-factual analysis, where landscape covariates can be modified to represent a disturbance, management action, reserve or habitat corridor design, and trajectories can be simulated to understand how animals may respond by changing their movement dynamics, habitat selection or connectivity (Hofmann et al., 2023). Other applications include running near-term trajectories that assess the likelihood of an area being used by an animal in the future, which may be useful to assess colonisation and invasion potential of introduced species (Lustig et al., 2017; Lustig et al., 2019; Patterson et al., 2024), or to plan upcoming management when the locations of animals are currently known. Trajectories from SSFs have already seen useful application for connectivity, and there is potential to identify movement corridors and understand metapopulation dynamics in fragmented environments (Hooker et al., 2021; Whittington et al., 2022; Aiello et al., 2023; Hofmann et al., 2023; Sells et al., 2023), particularly when combined with additional data such as genetics to assess historic connectivity (Lowe & Allendorf, 2010; Dussex et al., 2015).

An additional feature of parameterising trajectories using SSFs is that it can serve as the foundation for a more complex model (Hauenstein et al., 2019). Additional parameters that govern behavioural and ecological factors such as more sophisticated memory effects and home range behaviour, social interactions, and more flexible relationships between the animal and resource covariates can be added for a more sophisticated simulation model. The model would then need to be calibrated to data, but the SSF estimates for the movement and resource selection parameters can be used as priors, and approaches such as simulation-based inference can be used to fit the updated model to data (Hartig et al., 2011; Cranmer et al., 2020; Tejero-Cantero et al., 2020). For an example of this approach see Hauenstein et al. (2019). Here we have shown how summary statistics can be used to describe the characteristics of trajectories, which could form the basis of summary statistics for simulation-based inference, similar to the approach of Hauenstein et al. (2019).

5 Conclusions

Here we have incorporated temporal dynamics through harmonic terms into step selection models that we used to simulate trajectories. We found that dynamic models were more representative across our time-scale of model fitting. Adding temporal dynamics to the movement behaviour and memory processes also allowed for useful inference towards our study species, the invasive water buffalo (*Bubalus bubalis*), which can help to guide management operations in Northern Australia. As more ecologists are turning to SSFs to simulate trajectories for understanding future distribution and connectivity, we recommend incorporating temporal dynamics to more realistically represent animal behaviour through time, particularly over longer time-scales such as seasonal dynamics. For those wanting to better understand movement and habitat selection of their species, including temporal dynamics can provide richer information, particularly for species with clear daily or seasonal patterns of behaviour.

6 Data availability

Code and data are available at https://github.com/swforrest/dynamic_SSF_sims, including a walk-through of fitting harmonic terms in step selection models.

7 Acknowledgements

SWF was supported by an Australian Government Research Training Program Scholarship and a CSIRO top-up scholarship. CD was supported by an Australian Research Council Future Fellowship (FT210100260). This work was funded by the federal government's Department of Agriculture, Fisheries and Forestry under the Control tools and technologies for established pest animals and weeds competitive grants program and the Smart Farming Partnerships Program (round 2). Computational resources and services used in this work were provided by the eResearch Office, Queensland University of Technology, Brisbane, Australia. We thank Michael Lynch (Melbourne Zoo), Jack Larson and Patrick Carmody for their assistance in the capture and collaring of animals. The Ricky Archer and the Bawinanga Rangers for their support in all field activities. SWF thanks Charlotte Patterson and members of the Applied Mathematical Ecology (AMEG) and Bayesian Research and Applications Group (BRAG) for helpful discussions and feedback on the work.

8 Author Contributions

SWF, DP, JRP and AJH conceived the ideas and developed the modelling methodology; AJH, JP and EV designed the data collection and collected the data; SF analysed the data and led the writing of the manuscript. All authors contributed critically to the drafts and gave final approval for publication.

References

Abrahms, B., Seidel, D. P., Dougherty, E., Hazen, E. L., Bograd, S. J., Wilson, A. M., Weldon McNutt, J., Costa, D. P., Blake, S., Brashares, J. S., & Getz, W. M. (2017). Suite of simple metrics reveals common movement syndromes across vertebrate taxa. *Movement Ecology*, *5*(1), 12. https://doi.org/10.1186/s40462-017-0104-2

Ager, A. A., Johnson, B. K., Kern, J. W., & Kie, J. G. (2003). Daily and seasonal movements and habitat use by female rocky mountain elk and mule deer. *Journal of Mammalogy*, *84*(3), 1076–1088. https://doi.org/10.1644/BBa-020

Aiello, C. M., Galloway, N. L., Prentice, P. R., Darby, N. W., Hughson, D., & Epps, C. W. (2023). Movement models and simulation reveal highway impacts and mitigation opportunities for a metapopulation-distributed species. *Landscape Ecology*, *38*(4), 1085–1103. https://doi.org/10.1007/s10980-023-01600-6

Arce Guillen, R., Lindgren, F., Muff, S., Glass, T. W., Breed, G. A., & Schlägel, U. E. (2023). Accounting for unobserved spatial variation in step selection analyses of animal movement via spatial random effects. *Methods in Ecology and Evolution*. https://doi.org/10.1111/2041-210x.14208

Avgar, T., Baker, J. A., Brown, G. S., Hagens, J. S., Kittle, A. M., Mallon, E. E., McGreer, M. T., Mosser, A., Newmaster, S. G., Patterson, B. R., Reid, D. E. B., Rodgers, A. R., Shuter, J., Street, G. M., Thompson, I., Turetsky, M. J., Wiebe, P. A., & Fryxell, J. M. (2015). Space-use behaviour of woodland caribou based on a cognitive movement model. *The Journal of Animal Ecology*, *84*(4), 1059–1070. https://doi.org/10.1111/1365-2656.12357

Avgar, T., Deardon, R., & Fryxell, J. M. (2013). An empirically parameterized individual based model of animal movement, perception, and memory. *Ecological Modelling*, *251*, 158–172. https://doi.org/10.1016/j.ecolmodel.2012.12.002

Avgar, T., Potts, J. R., Lewis, M. A., & Boyce, M. (2016). Integrated step selection analysis: Bridging the gap between resource selection and animal movement. *Methods in Ecology and Evolution*, *7*(5), 619–630. https://doi.org/10.1111/2041-210x.12528

Barnett, A. H., & Moorcroft, P. R. (2008). Analytic steady-state space use patterns and rapid computations in mechanistic home range analysis. *Journal of Mathematical Biology*, *57*(1), 139–159. https://doi.org/10.1007/s00285-007-0149-8

Bastille-Rousseau, G., & Wittemyer, G. (2019). Leveraging multidimensional heterogeneity in resource selection to define movement tactics of animals. *Ecology Letters*, *22*(9), 1417–1427. https://doi.org/10.1111/ele.13327

Bastille-Rousseau, G., & Wittemyer, G. (2022). Simple metrics to characterize inter-individual and temporal variation in habitat selection behaviour. *The Journal of Animal Ecology*, *91*(8), 1693–1706. https://doi.org/10.1111/1365-2656.13738

Boyce, M., Pitt, J., Northrup, J. M., Morehouse, A. T., Knopff, K. H., Cristescu, B., & Stenhouse, G. B. (2010). Temporal autocorrelation functions for movement rates from global positioning system radiotelemetry data. *Philosophical Transactions of the Royal Society of London. Series B, Biological Sciences*, *365*(1550), 2213–2219. https://doi.org/10.1098/rstb.2010.0080

Braithwaite, R. W., Dudzinski, M. L., Ridpath, M. G., & Parker, B. S. (1984). The impact of water buffalo on the monsoon forest ecosystem in kakadu national park. *Austral Ecology*, *9*(4), 309–322. https://doi.org/10.1111/j.1442-9993.1984.tb01369.x

Brooks, M. E., Kristensen, K., van Benthem, K. J., Magnusson, A., Berg, C. W., Nielsen, A., Skaug, H. J., Mächler, M., & Bolker, B. M. (2017). glmmTMB balances speed and flexibility among packages for zero-inflated generalized linear mixed modeling. *The R Journal*, *9*(2), 378–400.

Campbell, H. A., Loewensteiner, D. A., Murphy, B. P., Pittard, S., & McMahon, C. R. (2020). Seasonal movements and site utilisation by asian water buffalo (bubalus bubalis) in tropical savannas and floodplains of northern australia. *Wildlife Research*, *48*(3), 230–239. https://doi.org/10.1071/WR20070

Craiu, R. V., Duchesne, T., Fortin, D., & Baillargeon, S. (2011). Conditional logistic regression with longitudinal follow-up and Individual-Level random coefficients: A stable and efficient Two-Step estimation method. *Journal of Computational and Graphical Statistics*, *20*(3), 767–784. https://doi.org/10.1198/jcgs.2011.09189

Craiu, R. V., Duchesne, T., Fortin, D., & Baillargeon, S. (2016). *R package 'TwoStepCLogit'. conditional logistic regression: A Two-Step estimation method* (tech. rep.).

Cranmer, K., Brehmer, J., & Louppe, G. (2020). The frontier of simulation-based inference. *Proceedings of the National Academy of Sciences of the United States of America*, *117*(48), 30055–30062. https://doi.org/10.1073/pnas.1912789117

Dall, S. R. X., Bell, A. M., Bolnick, D. I., & Ratnieks, F. L. W. (2012). An evolutionary ecology of individual differences (A. Sih, Ed.). *Ecology Letters*, *15*(10), 1189–1198. https://doi.org/10.1111/j.1461-0248.2012.01846.x

Duchesne, T., Fortin, D., & Rivest, L.-P. (2015). Equivalence between step selection functions and biased correlated random walks for statistical inference on animal movement. *PloS One*, *10*(4), e0122947. https://doi.org/10.1371/journal.pone.0122947

Dussex, N., Sainsbury, J., Moorhouse, R., Jamieson, I. G., & Robertson, B. C. (2015). Evidence for bergmann's rule and not allopatric subspeciation in the threatened kaka (nestor meridionalis). *The Journal of Heredity*, *106*(6), 679–691. https://doi.org/10.1093/jhered/esv079

Ellison, N., Potts, J. R., Strickland, B. K., Demarais, S., & Street, G. M. (2024). Combining animal interactions and habitat selection into models of space use: A case study with white-tailed deer. *Wildlife Biology*, e01211. https://doi.org/10.1002/wlb3.01211

Fagan, W. F., Lewis, M. A., Auger-Méthé, M., Avgar, T., Benhamou, S., Breed, G., LaDage, L., Schlägel, U. E., Tang, W.-W., Papastamatiou, Y. P., Forester, J., & Mueller, T. (2013). Spatial memory and animal movement. *Ecology Letters*, *16*(10), 1316–1329. https://doi.org/10.1111/ele.12165

Fieberg, J., Freeman, S., & Signer, J. (2023). *Evaluating goodness-of-fit of animal movement models using lineups*. https://doi.org/10.1101/2023.09.26.559591

Fieberg, J., Signer, J., Smith, B., & Avgar, T. (2021). A 'how to' guide for interpreting parameters in habitat-selection analyses. *The Journal of Animal Ecology*, *90*(5), 1027–1043. https://doi.org/10.1111/1365-2656.13441

Fleming, C. H., Fagan, W. F., Mueller, T., Olson, K. A., Leimgruber, P., & Calabrese, J. M. (2015). Rigorous home range estimation with movement data: A new autocorrelated kernel density estimator. *Ecology*, *96*(5), 1182–1188. https://doi.org/10.1890/14-2010.1

Forester, J. D., Im, H. K., & Rathouz, P. J. (2009). Accounting for animal movement in estimation of resource selection functions: Sampling and data analysis. *Ecology*, *90*(12), 3554–3565. https://doi.org/10.1890/08-0874.1

Forrest, S. W., Rodriguez-Recio, M., & Seddon, P. J. (2022). *Estimating home range and temporal space use variability reveals age-related differences in risk exposure for reintroduced parrots*. https://doi.org/10.1101/2022.12.17.520898

Fortin, D., Beyer, H. L., Boyce, M. S., Smith, D. W., Duchesne, T., & Mao, J. S. (2005). Wolves influence elk movements: Behavior shapes a trophic cascade in yellowstone national park. *Ecology*, *86*(5), 1320–1330. https://doi.org/10.1890/04-0953

Gitzen, R. A., Millspaugh, J. J., & Kernohan, B. J. (2006). Bandwidth selection for Fixed-Kernel analysis of animal utilization distributions. *Wildfire*, *70*(5), 1334–1344. https://doi.org/10.2193/0022-541X(2006)70[1334:BSFFAO]2.0.CO;2

Guisan, A., & Thuiller, W. (2005). Predicting species distribution: Offering more than simple habitat models. *Ecology Letters*, *8*(9), 993–1009. https://doi.org/10.1111/j.1461-0248.2005.00792.x

Guisan, A., Thuiller, W., & Zimmermann, N. E. (2017). *Habitat suitability and distribution models: With applications in R*. Cambridge University Press. https://doi.org/10.1017/9781139028271

Guisan, A., Tingley, R., Baumgartner, J. B., Naujokaitis-Lewis, I., Sutcliffe, P. R., Tulloch, A. I. T., Regan, T. J., Brotons, L., McDonald-Madden, E., Mantyka-Pringle, C., Martin, T. G., Rhodes, J. R., Maggini, R., Setterfield, S. A., Elith, J., Schwartz, M. W., Wintle, B. A., Broennimann, O., Austin, M., … Buckley, Y. M. (2013). Predicting species distributions for conservation decisions (H. Arita, Ed.). *Ecology Letters*, *16*(12), 1424–1435. https://doi.org/10.1111/ele.12189

Hanks, E. M., Hooten, M. B., & Alldredge, M. W. (2015). Continuous-time discrete-space models for animal movement. *The Annals of Applied Statistics*, *9*(1), 145–165. https://doi.org/10.1214/14-AOAS803

Hartig, F., Calabrese, J. M., Reineking, B., Wiegand, T., & Huth, A. (2011). Statistical inference for stochastic simulation models–theory and application. *Ecology Letters*, *14*(8), 816–827. https://doi.org/10.1111/j.1461-0248.2011.01640.x

Hauenstein, S., Fattebert, J., Grüebler, M. U., Naef-Daenzer, B., Pe'er, G., & Hartig, F. (2019). Calibrating an individual-based movement model to predict functional connectivity for little owls. *Ecological Applications*, *29*(4), e01873. https://doi.org/10.1002/eap.1873

Haydon, D. T., Morales, J. M., Yott, A., Jenkins, D. A., Rosatte, R., & Fryxell, J. M. (2008). Socially informed random walks: Incorporating group dynamics into models of population spread and growth. *Proceedings. Biological sciences / The Royal Society*, *275*(1638), 1101–1109. https://doi.org/10.1098/rspb.2007.1688

Hijmans, R. J. (2024). Spatial data analysis [r package terra version 1.7-71].

Hofmann, D. D., Cozzi, G., McNutt, J. W., Ozgul, A., & Behr, D. M. (2023). A three-step approach for assessing landscape connectivity via simulated dispersal: African wild dog case study. *Landscape Ecology*, *38*(4), 981–998. https://doi.org/10.1007/s10980-023-01602-4

Hooker, M. J., Clark, J., Bond, B. T., & Chamberlain, M. J. (2021). Evaluation of connectivity among american black bear populations in georgia. *The Journal of Wildlife Management*, *85*(5), 979–988. https://doi.org/10.1002/jwmg.22041

Horn, B. K. P. (1981). Hill shading and the reflectance map. *Proceedings of the IEEE*, *69*(1), 14–47. https://doi.org/10.1109/PROC.1981.11918

Kays, R., Hirsch, B., Caillaud, D., Mares, R., Alavi, S., Havmøller, R. W., & Crofoot, M. (2023). Multi-scale movement syndromes for comparative analyses of animal movement patterns. *Movement Ecology*, *11*(1), 61. https://doi.org/10.1186/s40462-022-00365-y

Kie, J. G. (2013). A rule-based ad hoc method for selecting a bandwidth in kernel home-range analyses. *Animal Biotelemetry*, *1*(1), 1–12. https://doi.org/10.1186/2050-3385-1-13

Kim, D., Thompson, P. R., Wolfson, D., Merkle, J., Oliveira-Santos, L. G. R., Forester, J. D., Avgar, T., Lewis, M. A., & Fieberg, J. (2023). *Identifying signals of memory from observations of animal movements in plato's cave*. https://doi.org/10.1101/2023.08.15.553411

Klappstein, N. J., Thomas, L., & Michelot, T. (2023). Flexible hidden markov models for behaviour-dependent habitat selection. *Movement Ecology*, *11*(1), 30. https://doi.org/10.1186/s40462-023-00392-3

Klappstein, N., Michelot, T., Fieberg, J., Pedersen, E., Field, C., & Flemming, J. M. (2024). *Step selection analysis with non-linear and random effects in mgcv*. https://doi.org/10.1101/2024.01.05.574363

Le Goff, M., Hendrix, J. G., Webber, Q. M. R., Robitaille, A. L., & Vander Wal, E. (2023). Environmental, social and morphological drivers of fission–fusion dynamics in a social ungulate. *Animal Behaviour*. https://doi.org/10.1016/j.anbehav.2023.10.014

Lowe, W. H., & Allendorf, F. W. (2010). What can genetics tell us about population connectivity? *Molecular Ecology*, *19*(15), 3038–3051. https://doi.org/10.1111/j.1365-294X.2010.04688.x

Lustig, A., James, A., Anderson, D., & Plank, M. (2019). Pest control at a regional scale: Identifying key criteria using a spatially explicit, agent-based model. *The Journal of Applied Ecology*, *56*(7), 1515–1527. https://doi.org/10.1111/1365-2664.13387

Lustig, A., Worner, S. P., Pitt, J. P. W., Doscher, C., Stouffer, D. B., & Senay, S. D. (2017). A modeling framework for the establishment and spread of invasive species in heterogeneous

environments. *Ecology and Evolution*, *7*(20), 8338–8348. https://doi.org/10.1002/ece3.2915

McClintock, B. T., King, R., Thomas, L., Matthiopoulos, J., McConnell, B. J., & Morales, J. M. (2012). A general discrete-time modeling framework for animal movement using multistate random walks. *Ecological Monographs*, *82*(3), 335–349. https://doi.org/10.1890/11-0326.1

McElreath, R. (2020). *Statistical rethinking: A bayesian course with examples in R and stan*. Chapman & Hall. https://doi.org/10.1201/9780429029608/statistical-rethinking-richard-mcelreath

McMahon, C. R., & Bradshaw, C. J. A. (2008). To catch a buffalo: Field immobilisation of asian swamp buffalo using etorphine and xylazine. *Australian Veterinary Journal*, *86*(6), 235–241. https://doi.org/10.1111/j.1751-0813.2008.00303.x

Merkle, J. A., Fortin, D., & Morales, J. M. (2014). A memory-based foraging tactic reveals an adaptive mechanism for restricted space use. *Ecology Letters*, *17*(8), 924–931. https://doi.org/10.1111/ele.12294

Merkle, J. A., Potts, J. R., & Fortin, D. (2017). Energy benefits and emergent space use patterns of an empirically parameterized model of memory-based patch selection. *Oikos*, *126*(2). https://doi.org/10.1111/oik.03356

Merkle, J. A., Sawyer, H., Monteith, K. L., Dwinnell, S. P. H., Fralick, G. L., & Kauffman, M. J. (2019). Spatial memory shapes migration and its benefits: Evidence from a large herbivore. *Ecology Letters*, *22*(11), 1797–1805. https://doi.org/10.1111/ele.13362

Michelot, T., Klappstein, N. J., Potts, J. R., & Fieberg, J. (2024). Understanding step selection analysis through numerical integration. *Methods in Ecology and Evolution*, *15*(1), 24–35. https://doi.org/10.1111/2041-210x.14248

Mihailou, H., & Massaro, M. (2021). An overview of the impacts of feral cattle, water buffalo and pigs on the savannas, wetlands and biota of northern australia. *Austral Ecology*, *46*(5), 699–712. https://doi.org/10.1111/aec.13046

Muff, S., Signer, J., & Fieberg, J. (2020). Accounting for individual-specific variation in habitat-selection studies: Efficient estimation of mixed-effects models using bayesian or frequentist computation (E. V. Wal, Ed.). *The Journal of Animal Ecology*, *89*(1), 80–92. https://doi.org/10.1111/1365-2656.13087

Myneni, R. B., Hall, F. G., Sellers, P. J., & Marshak, A. L. (1995). The interpretation of spectral vegetation indexes. *IEEE Transactions on Geoscience and Remote Sensing*, *33*(2), 481–486. https://doi.org/10.1109/TGRS.1995.8746029

Nathan, R., Getz, W. M., Revilla, E., Holyoak, M., Kadmon, R., Saltz, D., & Smouse, P. E. (2008). A movement ecology paradigm for unifying organismal movement research. *Proceedings of the National Academy of Sciences of the United States of America*, *105*(49), 19052–19059. https://doi.org/10.1073/pnas.0800375105

Northrup, J. M., Vander Wal, E., Bonar, M., Fieberg, J., Laforge, M. P., Leclerc, M., Prokopenko, C. M., & Gerber, B. D. (2022). Conceptual and methodological advances in habitat-selection modeling: Guidelines for ecology and evolution. *Ecological Applications*, *32*(1), e02470. https://doi.org/10.1002/eap.2470

Oliveira-Santos, L. G. R., Forester, J. D., Piovezan, U., Tomas, W. M., & Fernandez, F. A. S. (2016). Incorporating animal spatial memory in step selection functions. *The Journal of Animal Ecology*, *85*(2), 516–524. https://doi.org/10.1111/1365-2656.12485

Osipova, L., Okello, M. M., Njumbi, S. J., Ngene, S., Western, D., Hayward, M. W., & Balkenhol, N. (2019). Using step-selection functions to model landscape connectivity for african elephants: Accounting for variability across individuals and seasons. *Animal Conservation*, *22*(1), 35–48. https://doi.org/10.1111/acv.12432

Patterson, C. R., Lustig, A., Seddon, P. J., Wilson, D. J., & van Heezik, Y. (2024). Eradicating an invasive mammal requires local elimination and reduced reinvasion from an urban source population. *Ecological Applications*, e2949. https://doi.org/10.1002/eap.2949

Petty, A. M., Werner, P. A., Lehmann, C. E. R., Riley, J. E., Banfai, D. S., & Elliott, L. P. (2007). Savanna responses to feral buffalo in kakadu national park, australia. *Ecological Monographs*, *77*(3), 441–463. https://doi.org/10.1890/06-1599.1

Picardi, S., Ranc, N., Smith, B. J., Coates, P. S., Mathews, S. R., & Dahlgren, D. K. (2021). Individual variation in temporal dynamics of post-release habitat selection. *Frontiers in Conservation Science*, *2*. https://doi.org/10.3389/fcosc.2021.703906

Pohle, J., Signer, J., Eccard, J. A., Dammhahn, M., & Schlägel, U. E. (2023). How to account for behavioural states in step-selection analysis: A model comparison.

Potts, J. R., Bastille-Rousseau, G., Murray, D. L., Schaefer, J. A., & Lewis, M. A. (2014). Predicting local and non-local effects of resources on animal space use using a mechanistic step

selection model. *Methods in Ecology and Evolution*, *5*(3), 253–262. https://doi.org/10.1111/2041-210X.12150

Potts, J. R., & Börger, L. (2023). How to scale up from animal movement decisions to spatiotemporal patterns: An approach via step selection. *The Journal of Animal Ecology*, *92*(1), 16–29. https://doi.org/10.1111/1365-2656.13832

Potts, J. R., Börger, L., Strickland, B. K., & Street, G. M. (2022). Assessing the predictive power of step selection functions: How social and environmental interactions affect animal space use. *Methods in Ecology and Evolution*, *13*(8), 1805–1818. https://doi.org/10.1111/2041-210x.13904

Potts, J. R., Giunta, V., & Lewis, M. A. (2022). Beyond resource selection: Emergent spatio-temporal distributions from animal movements and stigmergent interactions. *Oikos*, *2022*(6), e09188. https://doi.org/10.1111/OIK.09188

Potts, J. R., & Schlägel, U. E. (2020). Parametrizing diffusion-taxis equations from animal movement trajectories using step selection analysis (L. Börger, Ed.). *Methods in Ecology and Evolution*, *11*(9), 1092–1105. https://doi.org/10.1111/2041-210X.13406

Rafiq, K., Jordan, N. R., Golabek, K., McNutt, J. W., Wilson, A., & Abrahms, B. (2023). Increasing ambient temperatures trigger shifts in activity patterns and temporal partitioning in a large carnivore guild. *Proceedings. Biological sciences / The Royal Society*, *290*(2010), 20231938. https://doi.org/10.1098/rspb.2023.1938

Reed, B. C., Brown, J. F., VanderZee, D., Loveland, T. R., Merchant, J. W., & Ohlen, D. O. (1994). Measuring phenological variability from satellite imagery. *Journal of Vegetation Science*, *5*(5), 703–714. https://doi.org/10.2307/3235884

Rheault, H., Anderson, C. R., Jr, Bonar, M., Marrotte, R. R., Ross, T. R., Wittemyer, G., & Northrup, J. M. (2021). Some memories never fade: Inferring Multi-Scale memory effects on habitat selection of a migratory ungulate using Step-Selection functions. *Frontiers in Ecology and Evolution*, *9*. https://doi.org/10.3389/fevo.2021.702818

Richter, L., Balkenhol, N., Raab, C., Reinecke, H., Meißner, M., Herzog, S., Isselstein, J., & Signer, J. (2020). So close and yet so different: The importance of considering temporal dynamics to understand habitat selection. *Basic and Applied Ecology*, *43*, 99–109. https://doi.org/10.1016/j.baae.2020.02.002

Robinson, C. J., Smyth, D., & Whitehead, P. J. (2005). Bush tucker, bush pets, and bush threats: Cooperative management of feral animals in australia's kakadu national park. *Conservation Biology*, *19*(5), 1385–1391. https://doi.org/10.1111/j.1523-1739.2005.00196.x

Rue, H., Martino, S., & Chopin, N. (2009). Approximate bayesian inference for latent gaussian models by using integrated nested laplace approximations. *Journal of the Royal Statistical Society. Series B, Statistical methodology*, *71*(2), 319–392. https://doi.org/10.1111/j.1467-9868.2008.00700.x

Schlägel, U. E., & Lewis, M. A. (2014). Detecting effects of spatial memory and dynamic information on animal movement decisions. *Methods in Ecology and Evolution*, *5*(11), 1236–1246. https://doi.org/10.1111/2041-210X.12284

Sells, S. N., Costello, C. M., Lukacs, P. M., Roberts, L. L., & Vinks, M. A. (2023). Predicted connectivity pathways between grizzly bear ecosystems in western montana. *Biological Conservation*, *284*, 110199. https://doi.org/10.1016/j.biocon.2023.110199

Sheather, S. J., & Jones, M. C. (1991). A reliable Data-Based bandwidth selection method for kernel density estimation. *Journal of the Royal Statistical Society. Series B, Statistical methodology*, *53*(3), 683–690.

Signer, J., Fieberg, J., Reineking, B., Schlägel, U., Smith, B., Balkenhol, N., & Avgar, T. (2023). Simulating animal space use from fitted integrated Step-Selection functions (iSSF). *Methods in Ecology and Evolution*. https://doi.org/10.1111/2041-210x.14263

Signer, J., Fieberg, J., & Avgar, T. (2017). Estimating utilization distributions from fitted step-selection functions. *Ecosphere*, *8*(4), e01771. https://doi.org/10.1002/ecs2.1771

Signer, J., & Fieberg, J. R. (2021). A fresh look at an old concept: Home-range estimation in a tidy world. *PeerJ*, *9*, e11031. https://doi.org/10.7717/peerj.11031

Silk, M. J., Croft, D. P., Tregenza, T., & Bearhop, S. (2014). The importance of fission-fusion social group dynamics in birds. *Ibis*, *156*(4), 701–715. https://doi.org/10.1111/ibi.12191

Skeat, A. J., East, T. J., & Corbett, L. K. (1996). Impact of feral water buffalo. In C. M. Finlayson & I. Von Oertzen (Eds.), *Landscape and vegetation ecology of the kakadu region, northern australia* (pp. 155–177). Springer Netherlands. https://doi.org/10.1007/978-94-009-0133-9_8

Street, G. M., Fieberg, J., Rodgers, A. R., Carstensen, M., Moen, R., Moore, S. A., Windels, S. K., & Forester, J. D. (2016). Habitat functional response mitigates reduced foraging

opportunity: Implications for animal fitness and space use. *Landscape Ecology*, *31*(9), 1939–1953. https://doi.org/10.1007/s10980-016-0372-z

Stuber, E. F., Carlson, B. S., & Jesmer, B. R. (2022). Spatial personalities: A meta-analysis of consistent individual differences in spatial behavior. *Behavioral Ecology*, *33*(3), 477–486. https://doi.org/10.1093/beheco/arab147

Tejero-Cantero, A., Boelts, J., Deistler, M., Lueckmann, J.-M., Durkan, C., Gonçalves, P., Greenberg, D., & Macke, J. (2020). Sbi: A toolkit for simulation-based inference. *Journal of Open Source Software*, *5*(52), 2505. https://doi.org/10.21105/joss.02505

Thompson, P. R., Derocher, A. E., Edwards, M. A., & Lewis, M. A. (2022). Detecting seasonal episodic-like spatio-temporal memory patterns using animal movement modelling. *Methods in Ecology and Evolution*, *13*(1), 105–120. https://doi.org/10.1111/2041-210x.13743

Thurfjell, H., Ciuti, S., & Boyce, M. (2014). Applications of step-selection functions in ecology and conservation. *Movement Ecology*, *2*(1), 4. https://doi.org/10.1186/2051-3933-2-4

Tsalyuk, M., Kilian, W., Reineking, B., & Getz, W. M. (2019). Temporal variation in resource selection of african elephants follows long-term variability in resource availability. *Ecological Monographs*, *89*(2), e01348. https://doi.org/10.1002/ecm.1348

Tulloch, D. G. (1970). Seasonal movements and distribution of the sexes in the water buffalo, bubalus bubalis, in the northern territory. *Australian Journal of Zoology*, *18*, 399–414.

Turchin, P. (1998). *Quantitative analysis of movement: Measuring and modeling population redistribution in animals and plants*. Sinauer Associates.

Warton, D. I. (2022). *Eco-Stats: Data analysis in ecology*. Springer International Publishing. https://doi.org/10.1007/978-3-030-88443-7

Werner, P. A. (2005). Impact of feral water buffalo and fire on growth and survival of mature savanna trees: An experimental field study in kakadu national park, northern australia. *Austral Ecology*, *30*(6), 625–647. https://doi.org/10.1111/j.1442-9993.2005.01491.x

Whittington, J., Hebblewhite, M., Baron, R. W., Ford, A. T., & Paczkowski, J. (2022). Towns and trails drive carnivore movement behaviour, resource selection, and connectivity. *Movement Ecology*, *10*(1), 17. https://doi.org/10.1186/s40462-022-00318-5

Wood, S. N. (2011). Fast stable restricted maximum likelihood and marginal likelihood estimation of semiparametric generalized linear models. *Journal of the Royal Statistical Society. Series B, Statistical methodology*, *73*(1), 3–36. https://doi.org/10.1111/j.1467-9868.2010.00749.x

Worton, B. J. (1989). Kernel methods for estimating the utilization distribution in home-range studies. *Ecology*, *70*(1), 164–168. https://doi.org/10.2307/1938423

Appendix A Previous space use density estimation

We used kernel density estimation (KDE) to estimate the utilisation density (UD) of previous locations, which we combined with a temporal decay component. To assess the distribution of memory parameters, and for if we wanted to fit SSF models to individuals separately, we estimated individual level parameters for previous space use density. The KDE bandwidth, σ must be estimated per individual, so for a population level bandwidth parameter, $\bar{\sigma}$, we used the mean. In our case the number of locations that we used per individual was similar, although for imbalanced numbers of locations a mean that was weighted by the number of locations might be more appropriate. Figure A1 shows the distribution of estimated KDE bandwidths, with the red line representing the mean, when using the 'reference' bandwidth estimator from the `amt` package (Worton, 1989; Gitzen et al., 2006; Kie, 2013; Signer & Fieberg, 2021). Figure A2 shows the distribution of the estimated temporal decay parameters, with the red line indicating the estimation of γ_{pop}, which was estimated from the data of all individuals simultaneously whilst using $\bar{\sigma}$.

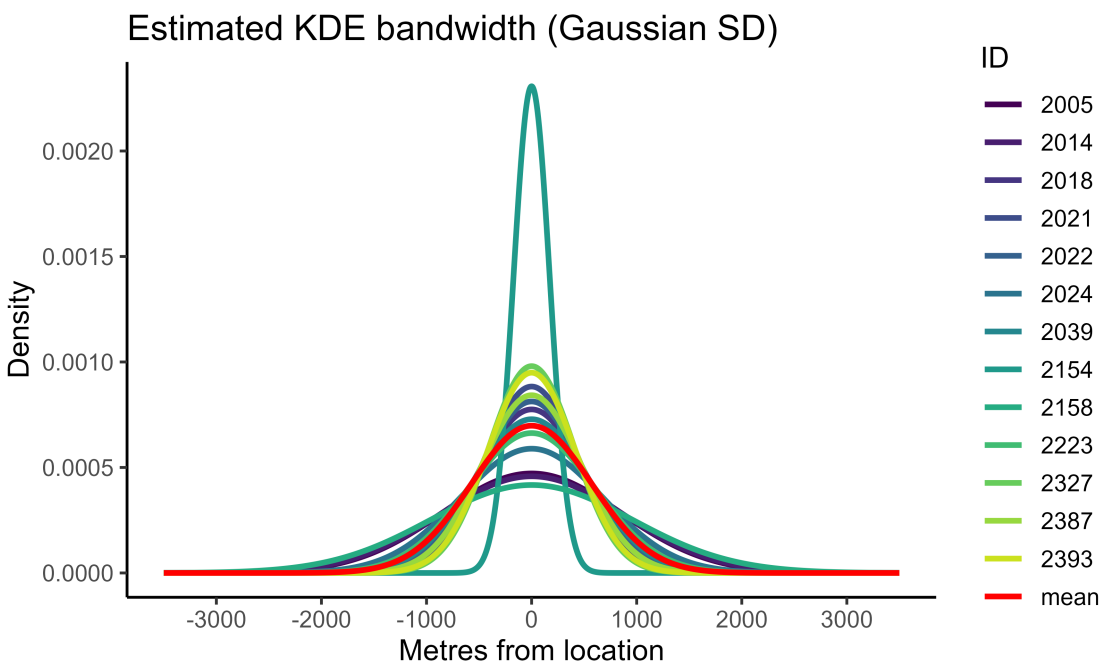

Figure A1: Estimated bandwidth for each individual buffalo using the reference bandwidth estimator in the 'amt' package (Signer et al., 2019; Signer & Fieberg, 2021). The same bandwidth was estimated and used in the x and y directions. Each line represents a different buffalo, and the red line shows the mean across individuals. All individuals besides one (ID 2154) had similar values of the KDE bandwidth. When simulating trajectories, we used the mean bandwidth as the standard deviation in the `dnorm` function, weighted by the temporal decay process using the γ_{pop} parameter that was estimated for all individuals simultaneously.

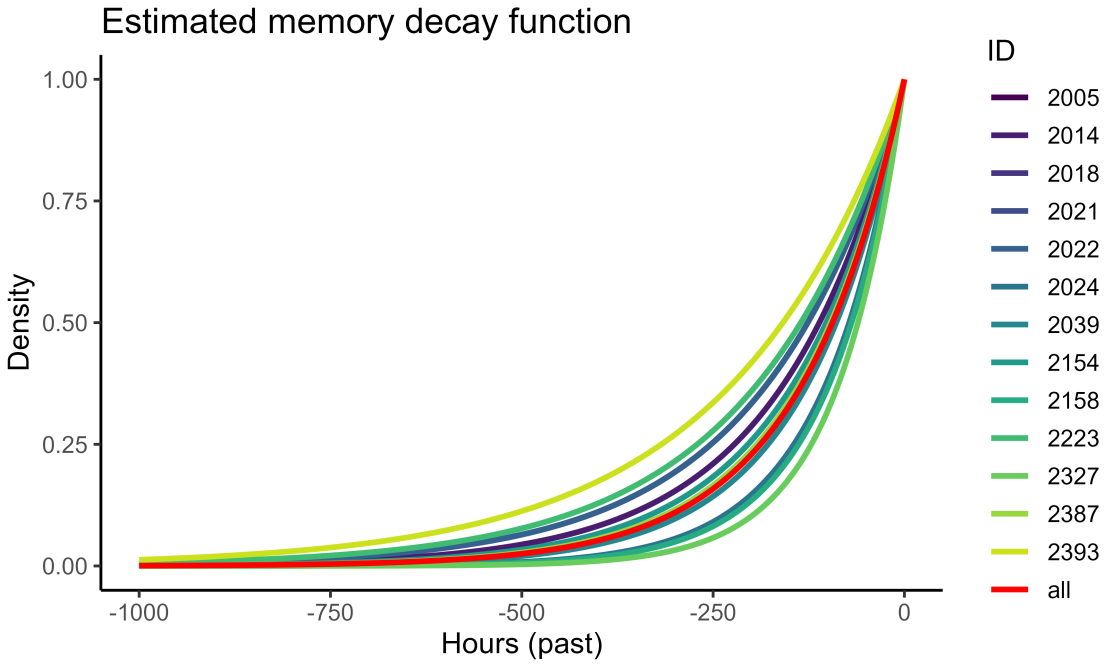

Figure A2: Estimated γ parameters of the negative exponential temporal decay component of the memory process. The x-axis shows the number of hours in the past, which does not include the most recent 24 hours. This period was ignored so the memory estimation does not conflate with the autocorrelation of movement. Each line represents a different buffalo, and the red line shows value of γ when optimising using the data from all individuals at once. When simulating trajectories, we used the mean bandwidth as the standard deviation in the `dnorm` function, weighted by the temporal decay process using the γ parameter that was estimated for all individuals simultaneously.

Appendix B Issues when updating temporally dynamic movement parameters

When fitting models to individuals separately, we had issues for some individuals where the movement parameter 'updating' (Avgar et al., 2016; Fieberg et al., 2021) resulted in impossibly large Gamma step length distributions. Using the inferred parameters of the step selection model, the updated Gamma scale parameter of the model, $\hat{q}$, which is defined as $\hat{q} = \frac{1}{(\frac{1}{q_0} - \beta_l)}$, where q_0 is the tentative scale parameter and β_l is the coefficient of the step length covariate, approached $\frac{1}{0}$, resulting in extremely large scale parameters. We also noticed that the scale parameter was accounting for the high variation in step lengths throughout the day, and the shape parameter remained relatively constant. The stability of the shape parameter suggests that the scale parameter is 'absorbing' the temporal variation, resulting in pathological results, although we also observed similar behaviour when using the exponential distribution, where only a single parameter is estimated. It is likely that further increasing the number of random steps will increase the accuracy of the numerical integration (Michelot et al., 2024), although even with 100 random steps we observed the pathological behaviour. For a high number of parameters and a large dataset increasing the number of steps beyond this can be computationally prohibitive, particularly when fitting models hierarchically. When using the TwoStep estimation for all individuals this was not an issue however, as it was only the model fits for some of the individuals when fitted separately that resulted in the pathological behaviour.

It is clear that this behaviour is due to the large difference between the 'tentative' step length and those that are estimated from the model due to the significant temporal changes. For other species that have less dynamic movement changes when compared to the buffalo this isn't likely to be an issue. The behaviour may also indicate an issue with harmonic terms, which are constrained by their sinusoidal behaviour, and may 'overshoot' at the modes (and approach $\frac{1}{0}$) in an attempt to accommodate sharp changes in movement behaviour, and either more harmonics that lend more flexibility, or an approach such as splines may lead to better results in these cases.

Appendix C Validations of simulations

To compare the complex movement trajectories, we used an animal-movement informed summary statistic approach to assess the simulated trajectories against the observed buffalo data (Abrahms et al., 2017; Hauenstein et al., 2019; Kays et al., 2023). We used a set of summary statistics that summarised the trajectory at each hour of the day (resulting in a single value per trajectory per hour), and a larger set of summary statistics that summarise the entire trajectory (resulting in a single value per trajectory). Following Kays et al. (2023), we selected summary statistics that we divided into categories relating to step metrics, path metrics and life-history metrics, but as we were fitting the models with habitat covariates, we also included a fourth category that we called habitat metrics, which assessed the distribution of locations in environmental space. The set of summary statistics that we selected were:

Hourly summary statistics

- Hourly mean, median and standard deviation of step length
- Hourly mean, median and standard deviation of NDVI
- Hourly mean and standard deviation of canopy cover (as it is a categorical variable the median was not as informative)
- Hourly mean and standard deviation of herbaceous vegetation
- Hourly mean, median and standard deviation of slope

Full trajectory summary statistics

Step measurements

- Mean step length
- Median step length
- Shape and scale of a Gamma distribution fitted to the step lengths
- Turn angle - concentration (k) of von Mises distribution

Path measurements

- Sinuosity
- Straightness

Life-history phase measurements

- Intensity of use, which is the total cumulative distance of the trajectory, divided by the square root of the total area, which is defined the Minimum Convex Polygon (MCP) surrounding 100% of the locations (Almeida et al., 2010).
- Mean turn angle correlation (Dray et al., 2010), where low values indicate high turn angle correlation (Abrahms et al., 2017).
- Mean residence time - the average number of hours an animal spends inside a circle of a given radius that is centred on each location without leaving the radius for more than a specified cut-off time (Barraquand & Benhamou, 2008). Similarly to Van Moorter et al. (2016) and Abrahms et al. (2017) we used the mean step length as the radius and 12 hours as the cut-off time.

- Total distance, which is the displacement from initial location (i.e. distance between the first and last locations)
- 50% area of the KDE utilisation distribution
- 95% area of the KDE utilisation distributions
- Monthly utilisation distribution overlap using Bhattacharyya's affinity, to assess stability of space use (higher values indicate more stable space use).

Habitat selection measurements

- Mean values of the distributions of all external covariates
- Standard deviation of the distributions of all external covariates

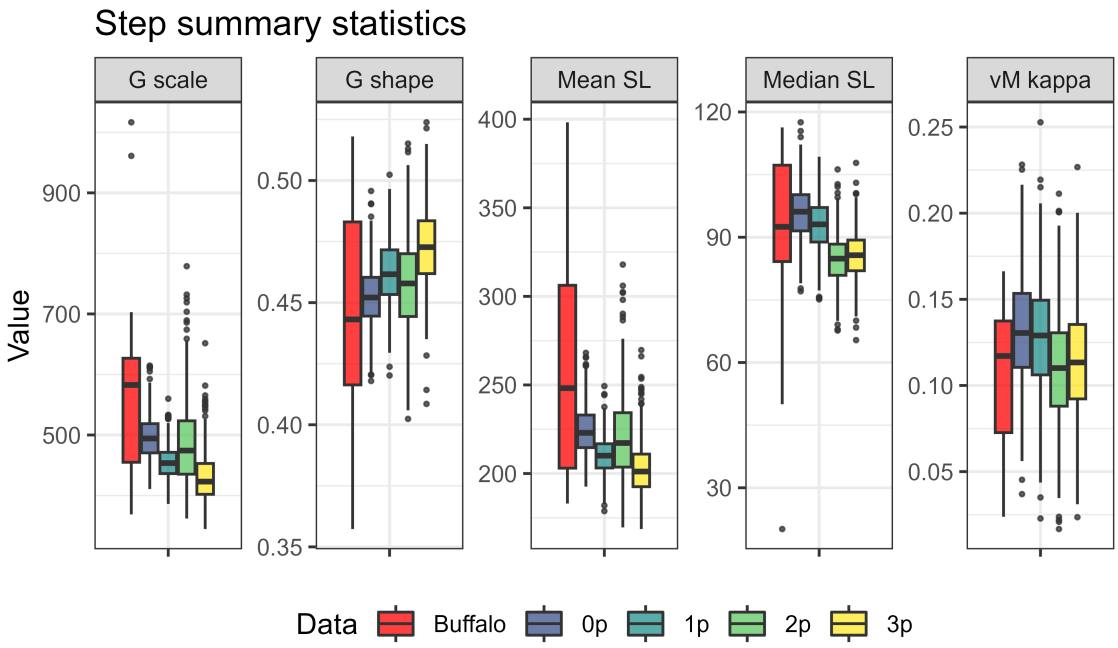

Figure A3: Summary statistics at the step level, where each data point that comprises the box plots represents a single observed (red, $n = 13$) or simulated trajectory. The G scale and G shape plots show the spread of scale and shape parameters of Gamma distributions that were fitted to the step lengths of observed (red) and simulated (0p, 1p, 2p and 3p) trajectories. The mean SL and median SL plots are the distributions of the mean and median step lengths for an entire observed or simulated trajectory. In this case the models with fewer harmonics tended to replicate the observed step lengths more accurately. The vM kappa plot shows the spread of von Mises kappa parameters estimated for each trajectory. The models with two and three pairs of harmonics (2p and 3p models) replicate the observed turning angles most accurately.

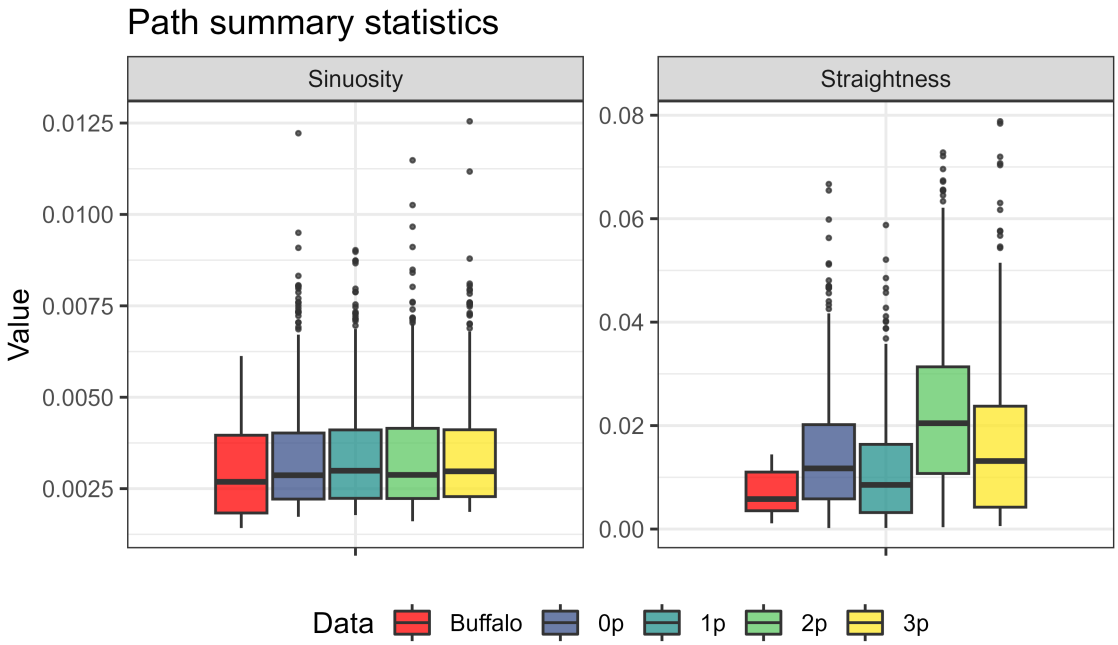

Figure A4: These plots show summary statistics at the path level, specifically the distribution of sinuosity and straightness values for each observed and simulated trajectory. Sinuosity values were similar for all observed and simulated trajectories, whereas the models with fewer harmonics tended to replicate the straightness index of the observed data marginally better.

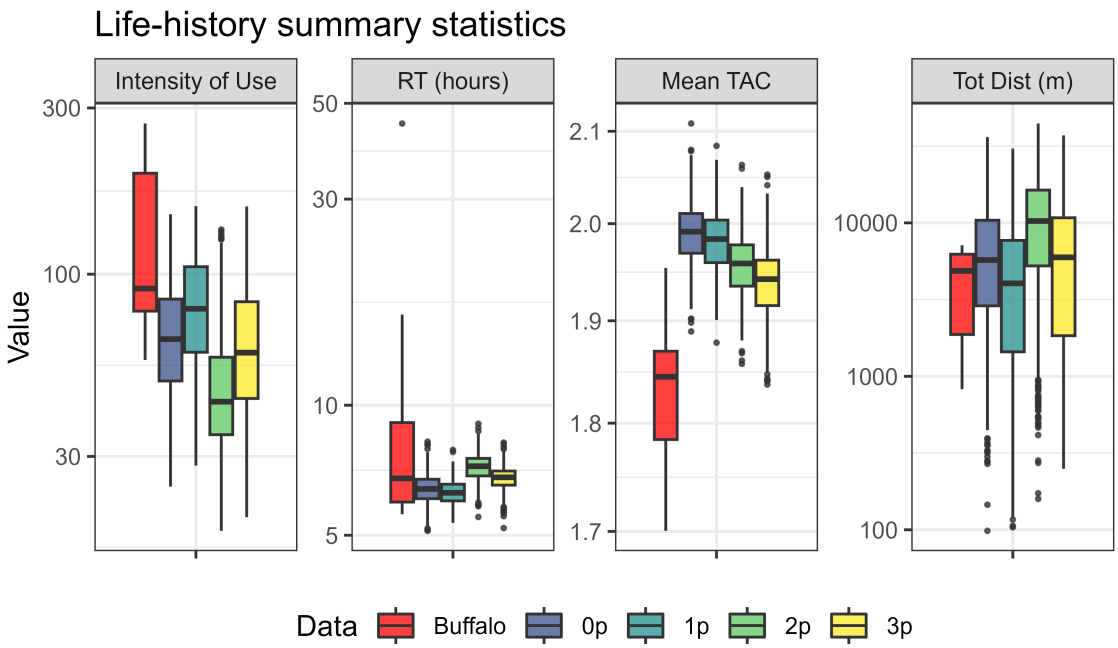

Figure A5: The assess how well the simulated trajectories captured the life-history characteristics of the observed trajectory (Abrahms et al., 2017; Kays et al., 2023), we calculated life-history summary statistics for the observed and simulated trajectories. The summaries were similar between all simulated trajectories, although models with fewer harmonics performed marginally better for how intensely the space was used and for the total distance from the first to the final location. Residence time was similar between simulated trajectories, and all were within the range of the observed data (but occupied a narrower range). Models with more harmonics performed better in terms of the turn-angle-correlation, although no models overlapped closely with the observed data.

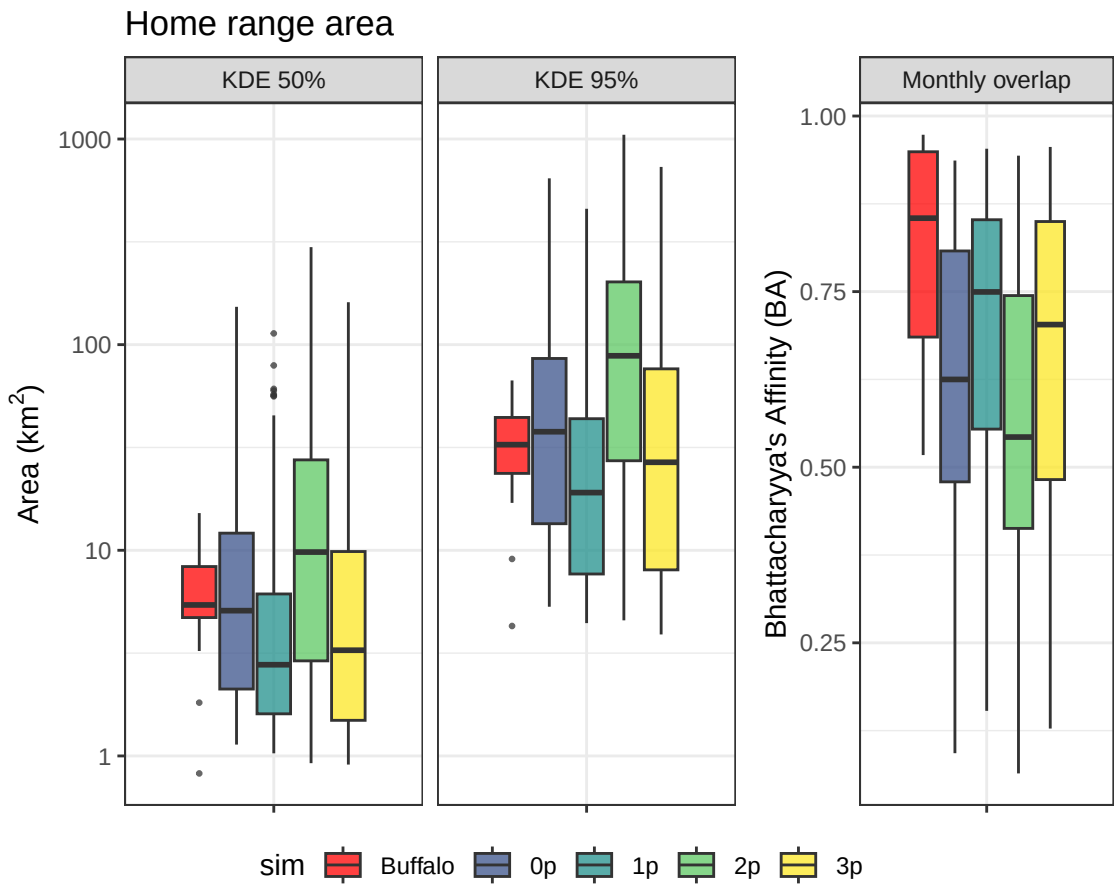

Figure A6: To assess how well the trajectories simulated from the step selection models capture the geographical space of the simulated trajectories, we used Kernel Density Estimation (KDE) with the 'reference' bandwidth estimator (Worton, 1989; Gitzen et al., 2006; Kie, 2013; Signer & Fieberg, 2021) to calculate the area contained within the 50% and 95% contours. We also compared the overlap of monthly space use using Bhattacharyya's Affinity (BA) between the observed (red) and simulated trajectories, to assess the stability of space use. The space use of the trajectories is sensitive to the parameterisation of the memory parameter, both with how previous space use density is estimated, and how it decays temporally, and the step selection model fit to derive a strength of association to previous space use density. Here we see that models with zero or three pairs of harmonics (0p and 3p) are most accurate when considering the area contained within the 95% contour of the KDE home range, and the trajectories from models with one or three pairs of harmonics (1p and 3p) are most accurate when considering the overlap between monthly KDE space use. Summarily, memory is a complex process, and providing higher flexibility to the model may allow for more accurate representations of geographical space use.

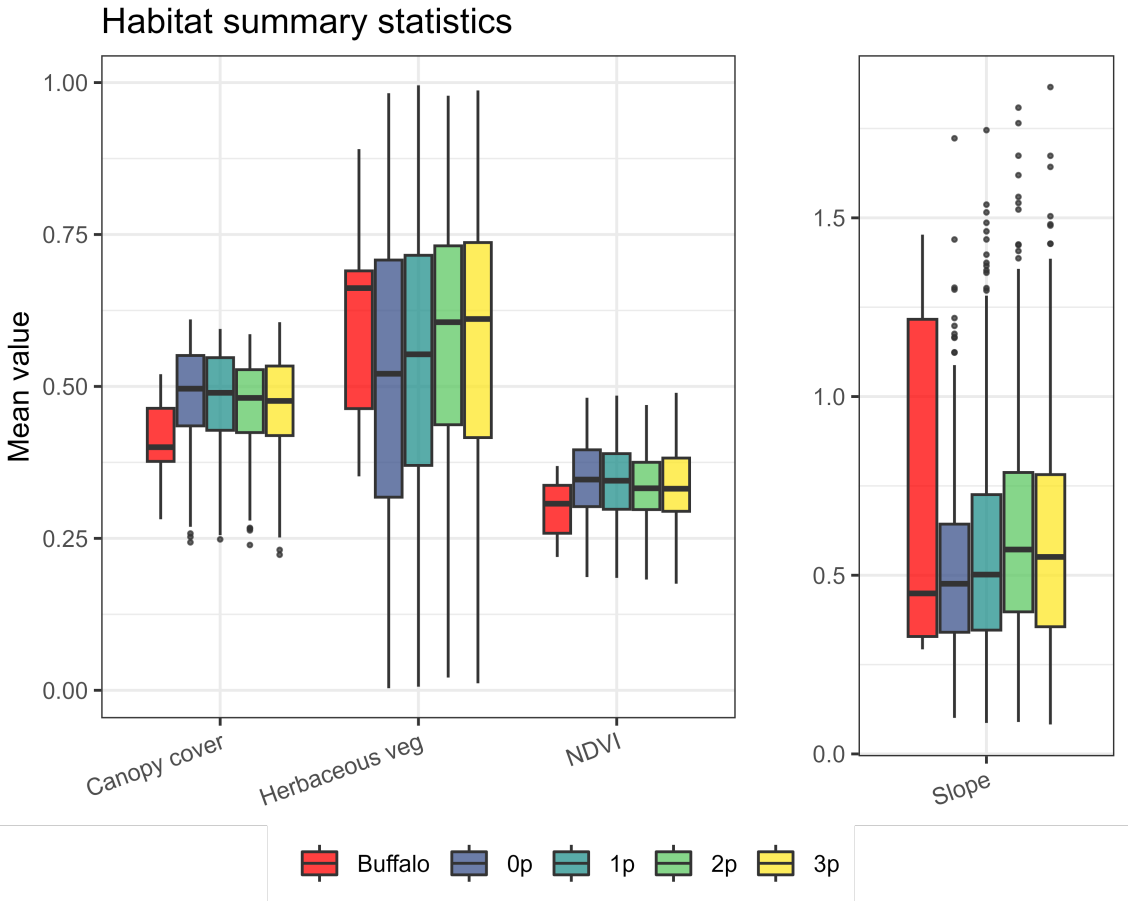

Figure A7: To assess the habitat selection over the entire trajectory, we extracted the values of the movement parameters and covariates for every location, and took the mean, median and standard deviation. Here we show the mean values, with a single data point per trajectory (observed or simulated), which comprise the boxplots. The observed buffalo data is shown in red. When considering the full trajectory, the average habitat selection behaviour is similar across the four different step selection models. The more dynamic models with two and three pairs of harmonics (2p and 3p) capture the selection of canopy cover, herbaceous vegetation and Normalised Difference Vegetation Index (NDVI) slightly more accurately and with slightly lower variance when compared to the observed buffalo data, although the differences are marginal. For slope the less dynamic models with zero or one pair of harmonics (0p and 1p) more closely capture the mean of slope, although this covariate did not strongly determine buffalo's step selection when compared the other covariates.

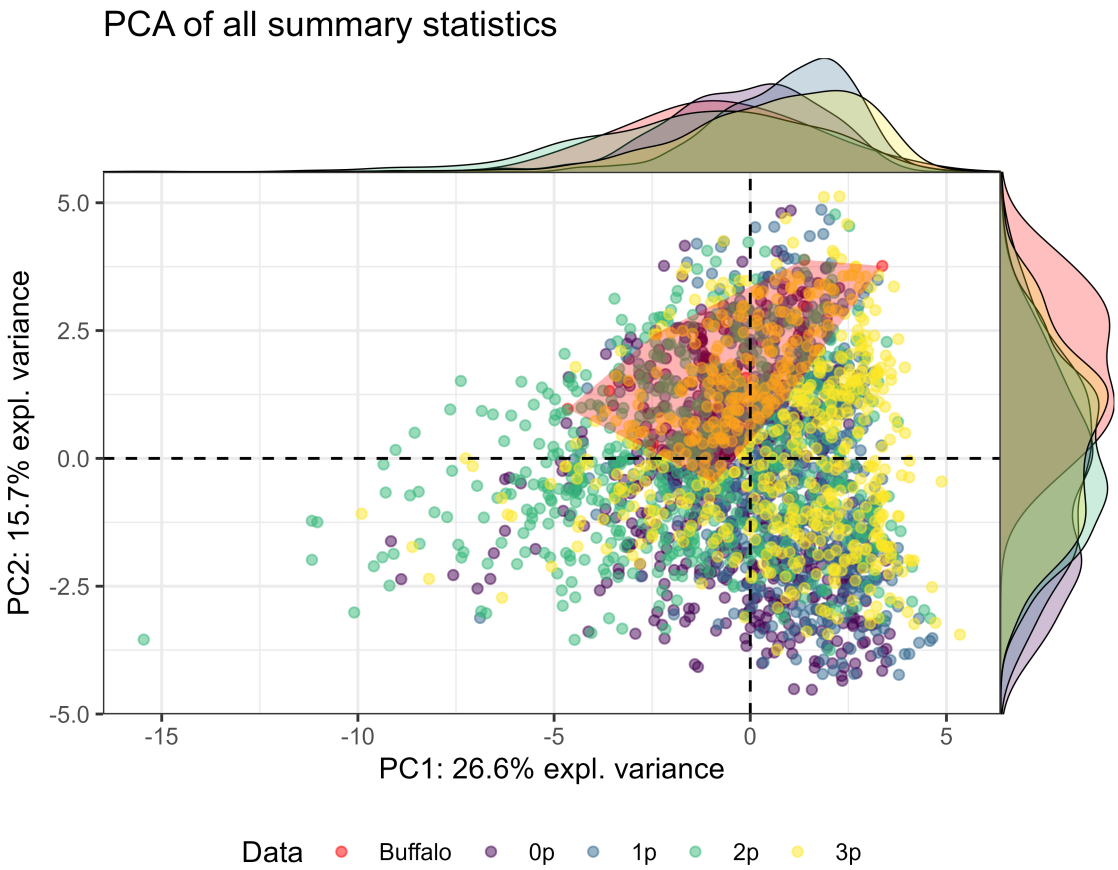

Figure A8: To reduce the dimensionality of the summary statistics and get an overall view of the ability of the simulations to capture the observed movement dynamics of the buffalo, we fitted a Principal Component Analysis (PCA) to all full-trajectory summaries (22 in total). In the first principal component axis, which explains 26.6% of the variance and is influenced mostly by the step and life-history summaries including the HR area, the models with zero and two pairs of harmonics most closely represent the observed data. Whereas in the second principal component axis, which explains 15.7% of the variance and is mostly influenced by the habitat selection summaries, the models with two and three pairs of harmonics most closely represent the observed data. It should be noted that all models perform well in replicating the characteristics of the observed data, and simpler models without quadratics for instance (not shown here), overlapped much less with the observed data.

References

Abrahms, B., Seidel, D. P., Dougherty, E., Hazen, E. L., Bograd, S. J., Wilson, A. M., Weldon McNutt, J., Costa, D. P., Blake, S., Brashares, J. S., & Getz, W. M. (2017). Suite of simple metrics reveals common movement syndromes across vertebrate taxa. *Movement Ecology*, *5*(1), 12. https://doi.org/10.1186/s40462-017-0104-2

Almeida, P. J. A. L., Vieira, M. V., Kajin, M., Forero-Medina, G., & Cerqueira, R. (2010). Indices of movement behaviour: Conceptual background, effects of scale and location errors. *Zoologia*, *27*(5), 674–680. https://doi.org/10.1590/S1984-46702010000500002

Avgar, T., Potts, J. R., Lewis, M. A., & Boyce, M. (2016). Integrated step selection analysis: Bridging the gap between resource selection and animal movement. *Methods in Ecology and Evolution*, *7*(5), 619–630. https://doi.org/10.1111/2041-210x.12528

Barraquand, F., & Benhamou, S. (2008). Animal movements in heterogeneous landscapes: Identifying profitable places and homogeneous movement bouts. *Ecology*, *89*(12), 3336–3348. https://doi.org/10.1890/08-0162.1

Dray, S., Royer-Carenzi, M., & Calenge, C. (2010). The exploratory analysis of autocorrelation in animal-movement studies. *Ecological Research*, *25*(3), 673–681. https://doi.org/10.1007/s11284-010-0701-7

Fieberg, J., Signer, J., Smith, B., & Avgar, T. (2021). A 'how to' guide for interpreting parameters in habitat-selection analyses. *The Journal of Animal Ecology*, *90*(5), 1027–1043. https://doi.org/10.1111/1365-2656.13441

Gitzen, R. A., Millspaugh, J. J., & Kernohan, B. J. (2006). Bandwidth selection for Fixed-Kernel analysis of animal utilization distributions. *Wildfire*, *70*(5), 1334–1344. https://doi.org/10.2193/0022-541X(2006)70[1334:BSFFAO]2.0.CO;2

Hauenstein, S., Fattebert, J., Grüebler, M. U., Naef-Daenzer, B., Pe'er, G., & Hartig, F. (2019). Calibrating an individual-based movement model to predict functional connectivity for little owls. *Ecological Applications*, *29*(4), e01873. https://doi.org/10.1002/eap.1873

Kays, R., Hirsch, B., Caillaud, D., Mares, R., Alavi, S., Havmøller, R. W., & Crofoot, M. (2023). Multi-scale movement syndromes for comparative analyses of animal movement patterns. *Movement Ecology*, *11*(1), 61. https://doi.org/10.1186/s40462-022-00365-y

Kie, J. G. (2013). A rule-based ad hoc method for selecting a bandwidth in kernel home-range analyses. *Animal Biotelemetry*, *1*(1), 1–12. https://doi.org/10.1186/2050-3385-1-13

Michelot, T., Klappstein, N. J., Potts, J. R., & Fieberg, J. (2024). Understanding step selection analysis through numerical integration. *Methods in Ecology and Evolution*, *15*(1), 24–35. https://doi.org/10.1111/2041-210x.14248

Signer, J., Fieberg, J., & Avgar, T. (2019). Animal movement tools (amt): R package for managing tracking data and conducting habitat selection analyses. *Ecology and Evolution*, *9*(2), 880–890. https://doi.org/10.1002/ece3.4823

Signer, J., & Fieberg, J. R. (2021). A fresh look at an old concept: Home-range estimation in a tidy world. *PeerJ*, *9*, e11031. https://doi.org/10.7717/peerj.11031

Van Moorter, B., Rolandsen, C. M., Basille, M., & Gaillard, J.-M. (2016). Movement is the glue connecting home ranges and habitat selection. *The Journal of Animal Ecology*, *85*(1), 21–31. https://doi.org/10.1111/1365-2656.12394

Worton, B. J. (1989). Kernel methods for estimating the utilization distribution in home-range studies. *Ecology*, *70*(1), 164–168. https://doi.org/10.2307/1938423